IS-T-389

MASTER

CONSTRUCTION OF A THREE CRYSTAL SPECTROMETER AND A STUDY OF THE DECAY OF ^{90}Nb

Ph. D. Thesis Submitted to Iowa State University, August 1970

S. Oliver Simmons

Ames Laboratory, USAEC

Iowa State University

Ames, Iowa 50010

PREPARED FOR THE U. S. ATOMIC ENERGY COMMISSION UNDER CONTRACT NO. W-7405-eng-82

Date Transmitted: October 1970

DISCLAIMER

IS-T-389

LEGAL NOTICE

Printed in the United States of America
Available from
Clearinghouse for Federal Scientific and Technical Information
National Bureau of Standards, U.S. Department of Commerce
Springfield, Virginia 22151
Price: Printed Copy $3.00; Microfiche $0.65

CONSTRUCTION OF A THREE CRYSTAL SPECTROMETER AND A STUDY OF THE DECAY OF ^{90}Nb

by

S. Oliver Simmons

A Dissertation Submitted to the
Graduate Faculty in Partial Fulfillment of
The Requirements for the Degree of
DOCTOR OF PHILOSOPHY

Major Subject: Nuclear Physics

Approved:

Allen B. Tacker
In Charge of Major Work

D. B. Marano
Head of Major Department

R. J. Gray
Dean of Graduate College

Iowa State University
Ames, Iowa

August 1970

CONSTRUCTION OF A THREE CRYSTAL SPECTROMETER AND A STUDY OF THE DECAY OF ^{90}Nb

S. Oliver Simmons

ABSTRACT

A gamma ray spectrometer consisting of a Ge(Li) detector partially surrounded by two NaI(Tl) scintillators has been constructed. The instrument has two modes of operation, the pair spectrometer mode for analyzing high energy gamma rays (above 1.022 MeV) and the Compton suppression mode for studying weak gamma rays in the presence of intense higher energy background radiation.

The decay of ^{90}Nb to levels in ^{90}Zr was investigated using the three crystal spectrometer in the Compton suppression mode to reduce background from the intense 2186 and 2319 keV transitions. Energies and absolute intensities of thirteen gamma ray transitions were determined. Using the K-conversion electron intensities from the work of other investigators and the gamma ray intensities from this work, conversion coefficients for the transitions were calculated. Comparison with theoretical values enabled deduction of the

multipolarities of most of the transitions.

The conventional shell model description of the levels of ^{90}Zr in terms of two protons in $(p\frac{1}{2})$ and $(g\frac{9}{2})$ orbitals is inconsistent with the observation of a strong E1 transition between the first 6^+ and 5^- levels. A calculation is presented which shows that this can be explained by mixing a 10^{-2}% component of $(g\frac{9}{2})(h\frac{11}{2})$ into the wavefunction for the 5^- state.

TABLE OF CONTENTS

I. INTRODUCTION

A. Spectrometer

In the late 1950's small semiconductor detectors were being used to analyze heavy particle spectra (1). The advent of thicker lithium-drift silicon detectors created better electron detectors (2, 3). One of the first attempts to make a lithium-drift silicon detector applicable to gamma ray studies was made by Chasman and Allen (4) in 1963. However, because of the small photoelectric cross section of silicon, these detectors were useful only at low energies (below 100 keV). Since the photoelectric cross section varies with atomic number Z and photon energy E as (5),

$$\sigma(Z,E) \propto Z^5 f(E),$$

higher Z semiconductor material suitable for lithium drifting were sought. The lithium-drift process was applied to germanium, which has a photoelectric cross section about forty times that of silicon, in 1962 (6). The first really useful Ge(Li) detector for analysis of gamma ray spectra over a large energy range was constructed in 1963 by Tavendale (7) and had a resolution approximately ten times better than a NaI(Tl) scintillation spectrometer.

Soon after the success in the construction of the lithium-drift germanium detector, Ewan and Tavendale (8)

reported using such a detector in a three crystal pair spectrometer. The germanium detector was placed between two NaI(Tl) scintillation spectrometers. The NaI(Tl) crystals were shielded from direct radiation from the source by lead. Only those pulses from the germanium detector that were in coincidence with detection of annihilation quanta in both NaI(Tl) detectors were recorded. Except for slight electronic modifications to allow for Compton suppression mode of operation this basic idea of the three crystal spectrometer is employed in the present study of the gamma ray decay of ^{90}Nb.

B. Theory

Periodicity in atomic properties has been known for over a century and was used to construct the periodic table of the elements. This phenomenon was attributed to the filling of successive shells by electrons in the atom under the influence of the Pauli principle.

From a study of the binding energies and abundances of nuclei, Elsasser in 1934 suggested that a similar periodicity exists in nuclear properties (9). Development of a theory was hampered by the lack of understanding of how the strong, short range nuclear force could be consistent with the long mean free path required for an atom-like orbital interpretation to be valid. In 1949, Mayer (10) and Haxel et al. (11) proposed a shell model theory that embodied the basic

assumption that each nucleon moves in an effective potential generated by all the other nucleons. Using the harmonic oscillator potential along with spin-orbit coupling in the Hamiltonian, Mayer (10) and Haxel et al. (11) were able to reproduce the observed periodicity in nuclear properties. A diagram of the shell model levels taken from Mayer and Jensen (12) is shown in Figure 1. The number of neutrons or protons needed to fill a major shell is called a "magic number". Because of the relatively large energy gap between a "magic number" orbital and the next allowed state, only particles above (or holes below) such levels are affected in low energy excitations. Consequently these particles (holes) will determine properties of the ground state and low-lying excited states.

The nucleus ^{90}Zr has 50 neutrons and 40 protons. From Figure 1 it can be seen that 50 neutrons fill all levels up to and including the $(1g\frac{9}{2})$ shell and that the next higher level, the $(1g\frac{7}{2})$ level, is separated from the $(1g\frac{9}{2})$ level by a large energy gap. Therefore for low energy excitations the 50 neutrons will remain inert.

The 40 protons fill all levels up to and including the $(2p\frac{1}{2})$ level. In 1955, Ford (13) suggested that the low-lying levels of ^{90}Zr could be accounted for by considering the last 2 protons to be in the $(2p\frac{1}{2})^2$, $(2p\frac{1}{2})(1g\frac{9}{2})$, and $(1g\frac{9}{2})^2$ configurations. The $(2p\frac{1}{2})^2$ configuration can

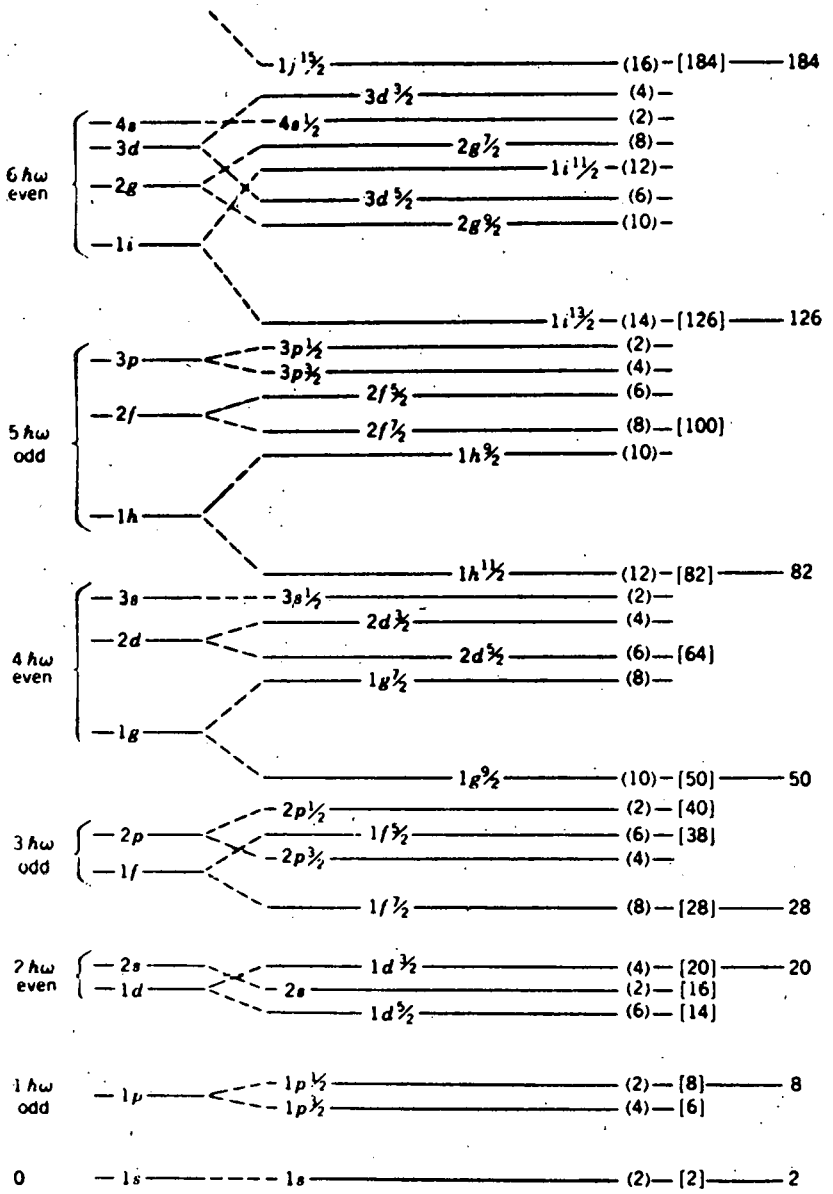

Figure 1. Single particle shell model levels

only give a 0^+ level. The $(2p\frac{1}{2})(1g\frac{9}{2})$ configuration can give levels of 4^- and 5^-. The $(1g\frac{9}{2})^2$ configuration can give levels of 0^+, 2^+, 4^+, 6^+, and 8^+. At the time Ford made his hypothesis only four levels of ^{90}Zr were known: 0^+ g.s., 0^+ at 1.75 MeV, 2^+ at 2.23 MeV and 5^- at 2.30 MeV. As more experimental data became available the other three levels (4^+, 6^+, and 8^+) belonging to the $(g\frac{9}{2})^2$ configuration were found (14).

Bayman et al. (15) in 1958 made detailed spectroscopic calculation based on levels arising from the three configurations proposed by Ford. These calculations were done using finite-range, spin-dependent, central forces. They assumed the single particle wave function to be those of a particle moving in a spherically symmetrical harmonic oscillator field and took the two body potential to be that of Yukawa in one case and a Gaussian in another case. In general the calculated spectra were in poor agreement with the experimental spectra. In 1960 Talmi and Unna (16), using a semi-empirical treatment, wereable to obtain good spectral fits by assuming that the potential energy of the nucleus was due to a two-body effective interaction between nucleons. The unknown matrix elements of those interactions, taken to be the same for all nuclei in which the same subshells were being filled, were determined by comparison with experimental data from ^{89}Y, ^{90}Zr, ^{91}Nb, ^{93}Tc, ^{87}Sr, ^{86}Sr and ^{85}Sr. In 1964, Auerbach and Talmi (17),

repeated the calculations of Talmi and Unna using more recent experimental data and obtained good spectral fits to the expanded data.

C. Experiment

The decay of ^{90}Nb has been studied by many investigators. In 1949 Kundu and Pool (18) identified ^{90}Nb by way of the nuclear reactions ^{90}Zr(d, 2n)^{90}Nb and ^{92}Mo(d, α)^{90}Nb. By absorption techniques they showed the existence of positrons with maximum energy of 1.19 MeV, gamma rays of 2.03 MeV and X-radiation following electron capture. Three years later Hollander et al. (19), using scintillation techniques, reported positrons with endpoint energy of 1.7 MeV and gamma ray energies of 2.23, 1.14 and 0.14 MeV. Using a double focusing spectrometer and a scintillation spectrometer, Hok et al. (20) in 1954 attributed to the decay of ^{90}Nb a positron spectrum consisting of three components with maximum energies of 1.500, 0.865 and 0.550 MeV and a total of seven gamma ray transitions. They proposed a decay scheme consisting of five excited states below 2.3 MeV. The first two excited states were placed at 1.13 and 1.27 MeV and both were assigned a spin and parity of 2^+. The third and fourth excited states were placed at 1.76 and 1.89 MeV and no spin or parity assignments were made for these levels. The fifth and last excited state was located at 2.20 MeV above the ground state

and had a spin and parity assignment of 1^-. The ground state of ^{90}Nb was placed only 3.79 MeV above the ground state of ^{90}Zr.

The discovery by Campbell et al. (21) in 1955 of a 2.3 MeV E5 ground state transition in ^{90}Zr from a 5^- isomeric level ($T_{1/2} = 0.83 \pm .03$ sec) was interpreted as evidence for a $(p\frac{1}{2})(g\frac{9}{2})$ state. Ford (13) observed that the predominant ground state E5 decay indicated the absence of excited states below 2 MeV with spin greater than zero, and predicted a 0^+ first excited state.

Further evidence for the existence of the 0^+ excited level in ^{90}Zr predicted by Ford (13) was found by Johnson et al. (22). Using a magnetic spectrometer and a strong source of ^{90}Y, they observed an internal conversion line corresponding to a transition of 1.75 MeV. A careful search for gamma rays with energies in the 1.75 MeV region produced a negative result. The 1.75 MeV transition was therefore assumed to be a monopole transition to the 0^+ ground state of ^{90}Zr.

An extensive study of the decay of ^{90}Nb was carried out by Sheline (14) in 1957. He determined the beta end point energy to be 1.48 ± 0.03 MeV. Nine gamma ray transitions were observed in the decay and placed in a decay scheme containing all the levels predicted by Ford (13) except the 4^- level. This work marked a great breakthrough in

establishing the low-lying levels in ^{90}Zr and in the placement of the gamma rays in the decay scheme. The decay scheme proposed by Sheline is shown in Figure 2.

Utilizing both single and coincident NaI(Tl) crystals and a magnetic spectrometer, Lazar et al. (23) in 1957 confirmed the findings of Sheline. They reported 13 gamma rays and determined conversion coefficients for five of the transitions. They also proposed three levels at 4.44, 5.05, and 5.45 MeV not previously reported. Their decay scheme is shown in Figure 3.

More recently Pettersson et al. (24) undertook a high resolution study of the decay of ^{90}Nb in an attempt to obtain information about levels above 3600 keV in ^{90}Zr. Using a double focusing iron yoke spectrometer and a Ge(Li) detector, they found 17 transitions in the internal conversion spectrum, six of which had not previously been observed. The Ge(Li) detector was mainly used to determine gamma ray intensities while the energies were determined from conversion electron measurements using the iron yoke spectrometer. Intense gamma rays at 1129, 2186, and 2319 keV produced sufficient Compton background to obscure photopeaks from many of the weaker, lower energy transitions. Thus they were unable to determine K-conversion coefficients for many of the weak transitions originating from the states above 3600 keV. They also measured the end-point energy of the intense

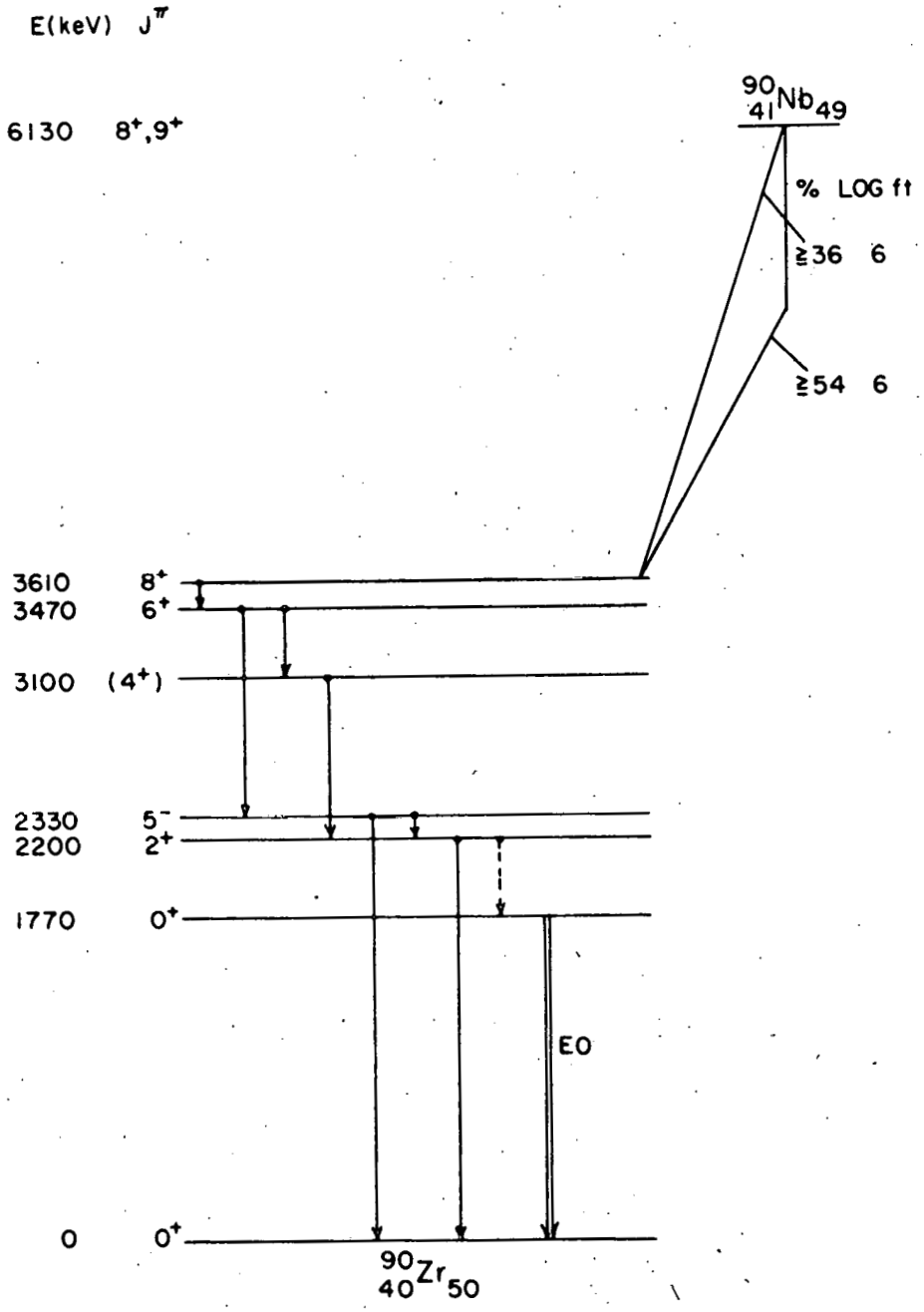

Figure 2. Decay scheme of ^{90}Nb proposed by Sheline

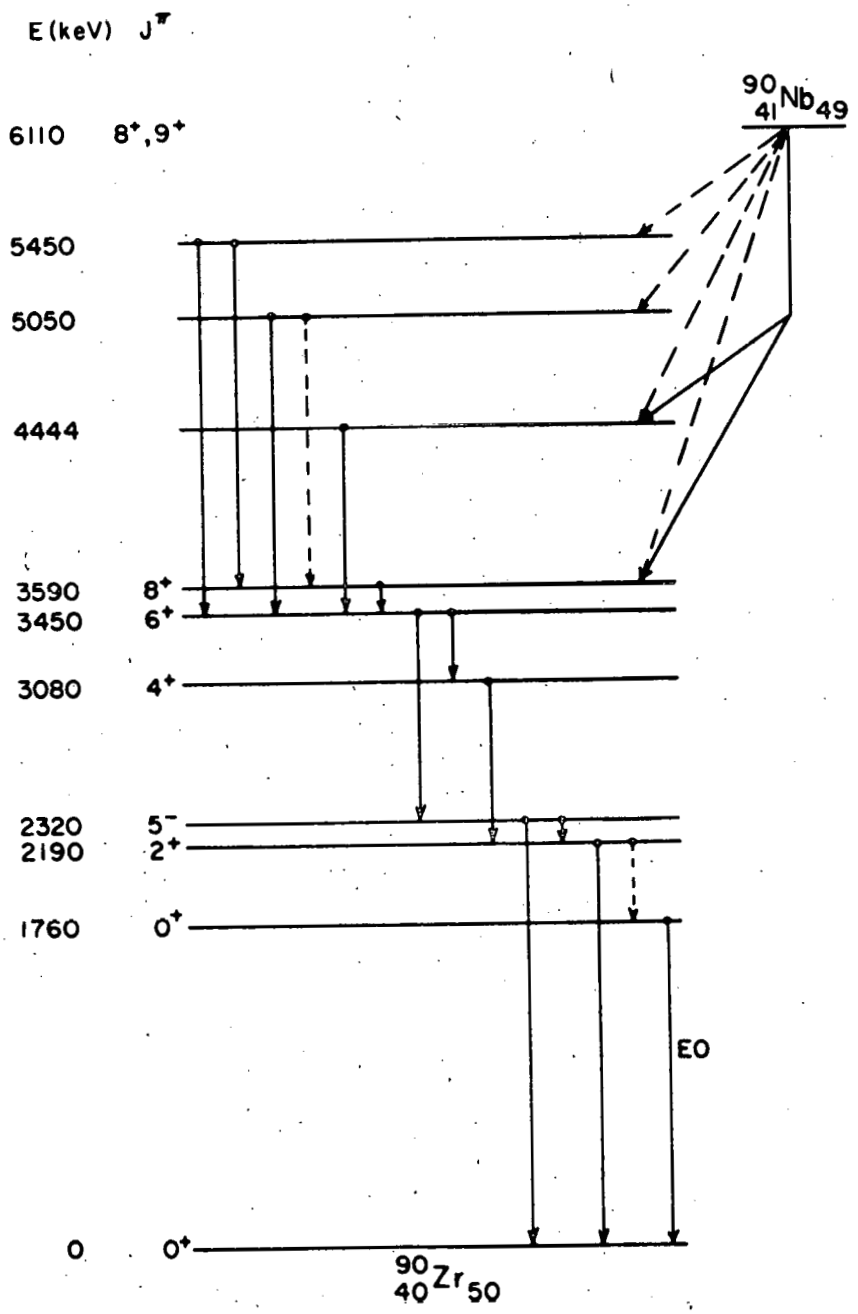

Figure 3. Decay scheme of ^{90}Nb proposed by Lazar *et al.*

(53 ± 6%) positron branch and determined the energy to be 1500 ± 4 keV, leading to a Q-value of 6111 ± 5 keV. The decay scheme proposed by Pettersson et al. is shown in Figure 4.

Nordheim's coupling rules (25, 26) suggest that the ground state of the odd-odd nucleus ^{90}Nb is either 8^+ or 9^+. In 1960 Brennan and Bernstein (27) proposed more precise coupling rules which suggest that the ground state of ^{90}Nb is an 8^+ state. An 8^+ ground state for ^{90}Nb is consistent with the recent work of Cooper et al. (28) on the decay of ^{90}Mo to states in ^{90}Nb.

Reaction studies by many investigators (29-34) reveal many more energy levels of ^{90}Zr than are populated in the decay of ^{90}Nb. Recently Ball (35) has summarized the extensive theoretical and experimental work on this isotope. Some of the ^{90}Zr levels excited by nuclear reaction are shown in Figure 5.

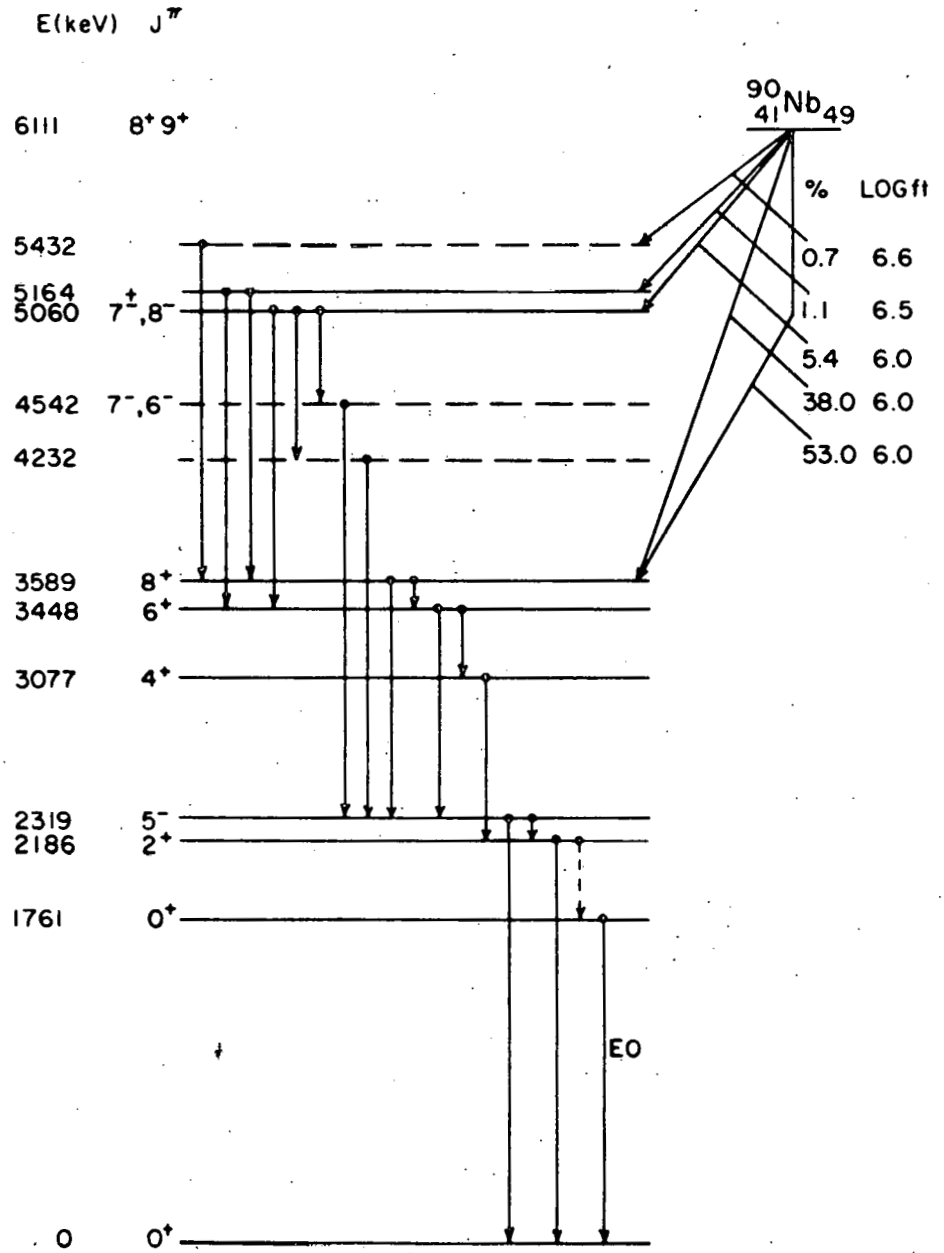

Figure 4. Decay scheme of ^{90}Nb proposed by Pettersson et al.

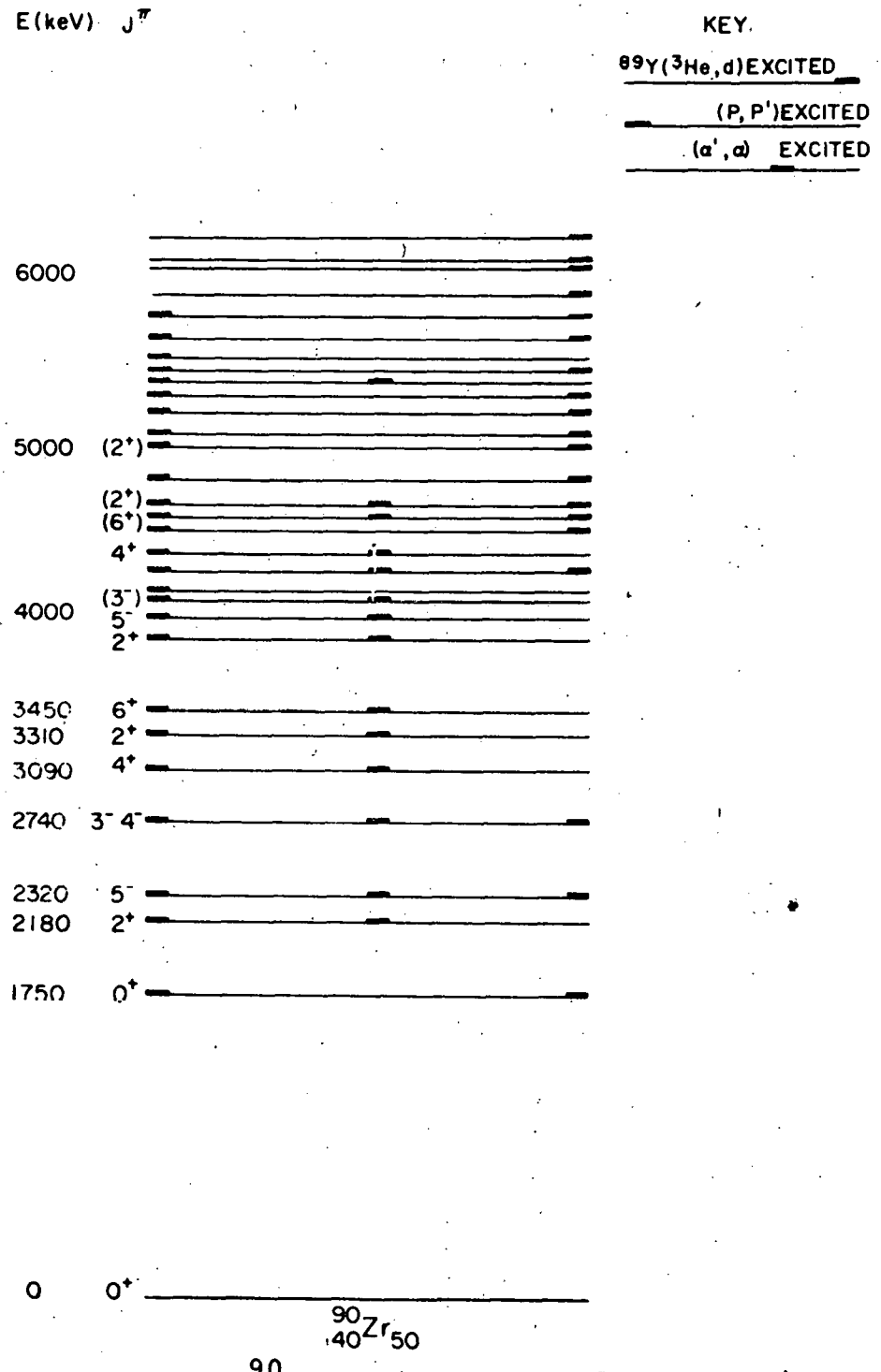

Figure 5. Levels of ^{90}Zr excited by nuclear reactions

II. CONSTRUCTION OF A THREE CRYSTAL SPECTROMETER

A. Gamma Ray Interactions

An ideal spectrometer would give a signal of unique amplitude for each gamma ray detected. Real detectors have a more complicated response which results in unwanted background. The three basic interactions by which the photons give up all or part of their energy in single events are: photoelectric effect, Compton scattering and pair production. A schematic representation of these three processes is shown in Figure 6. In the photoelectric effect the photon gives all of its energy to one electron. The electron in coming to rest gives up all of its acquired energy to the detector. Thus in the photoelectric effect all of the energy of the incident photon is absorbed in the detector. Such events give rise to photopeaks in the spectrum. This condition is illustrated in Figure 6(a).

In the Compton scattering process the gamma ray photon is scattered by an electron with an energy loss that depends on the angle of scattering. If the scattered photon escapes the detector, only a fraction of the energy of the incident gamma ray will be recorded. These events are responsible for Compton background in the spectrum. This process is illustrated in Figure 6(b).

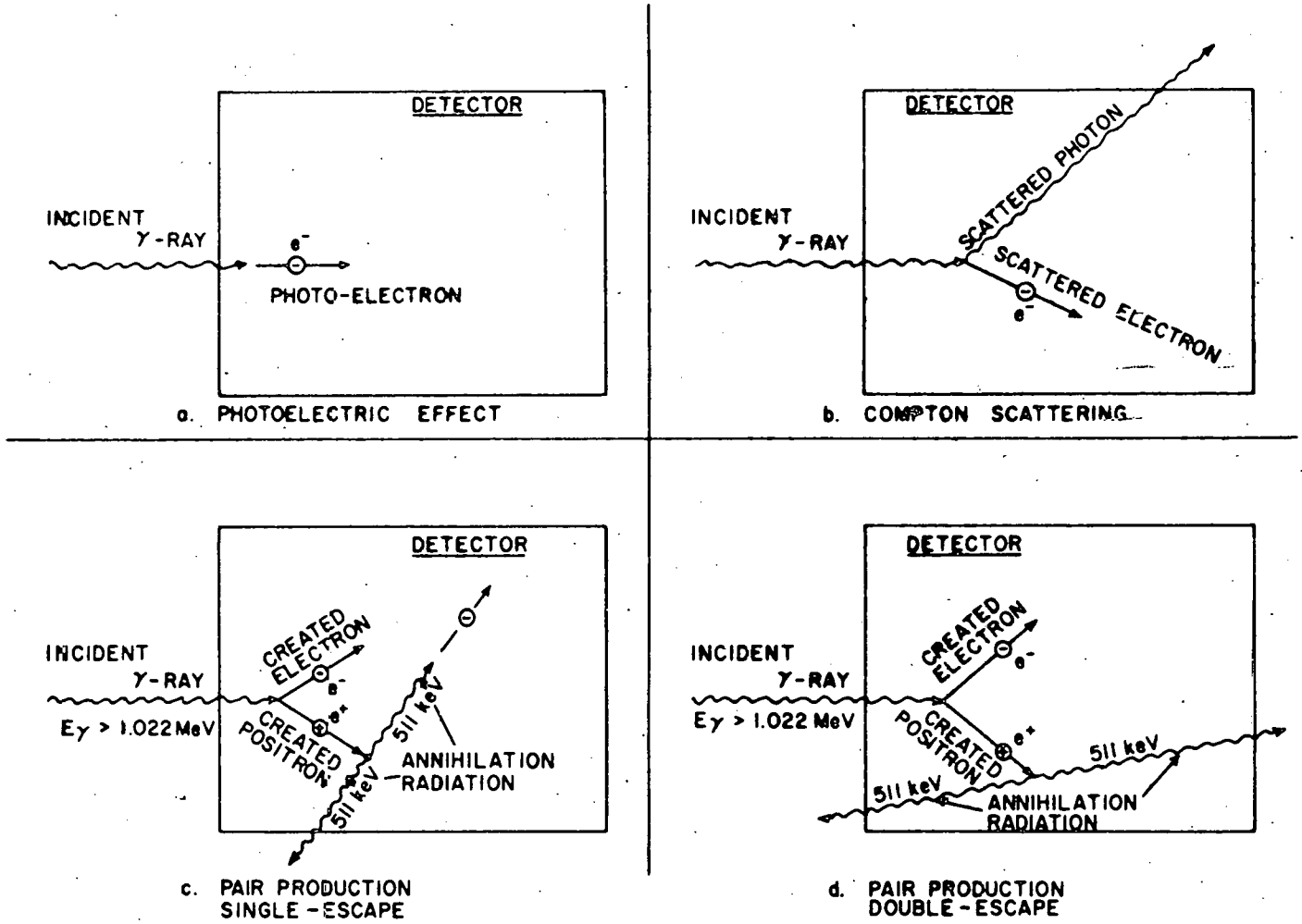

Figure 6. Gamma ray-detector interactions

In pair production a gamma ray photon with an energy greater than 1.022 MeV upon passing near a nucleus gives up all of its energy to the creation of an electron-positron pair with a kinetic energy equal to the energy of the incident photon minus the rest masses of an electron and positron (1.022 MeV). When the positron comes to rest it annihilates with an electron and emits two back-to-back 511 keV gamma rays. When only one 511 keV photon escapes from the detector, the energy absorbed by the detector is the energy of the incident photon minus 511 keV. This condition is termed "single-escape" and is illustrated in Figure 6(c). The resulting gamma ray peaks in the spectrum are called single-escape peaks. In a similar manner if both 511 keV photons escape from the detector the energy absorbed by the detector is the energy of the incident photon minus 1.022 MeV. This condition is termed "double-escape" and is illustrated in Figure 6(d). The resulting gamma ray peaks in the spectrum are called double-escape peaks.

B. Detector Configuration

The three crystal spectrometer is an instrument capable of reducing background in the recorded spectrum of pulses from the detector caused by the competing processes described above. A cutaway side view of the spectrometer is shown in Figure 7. The central detector, an Ortec Model 8101-20 high

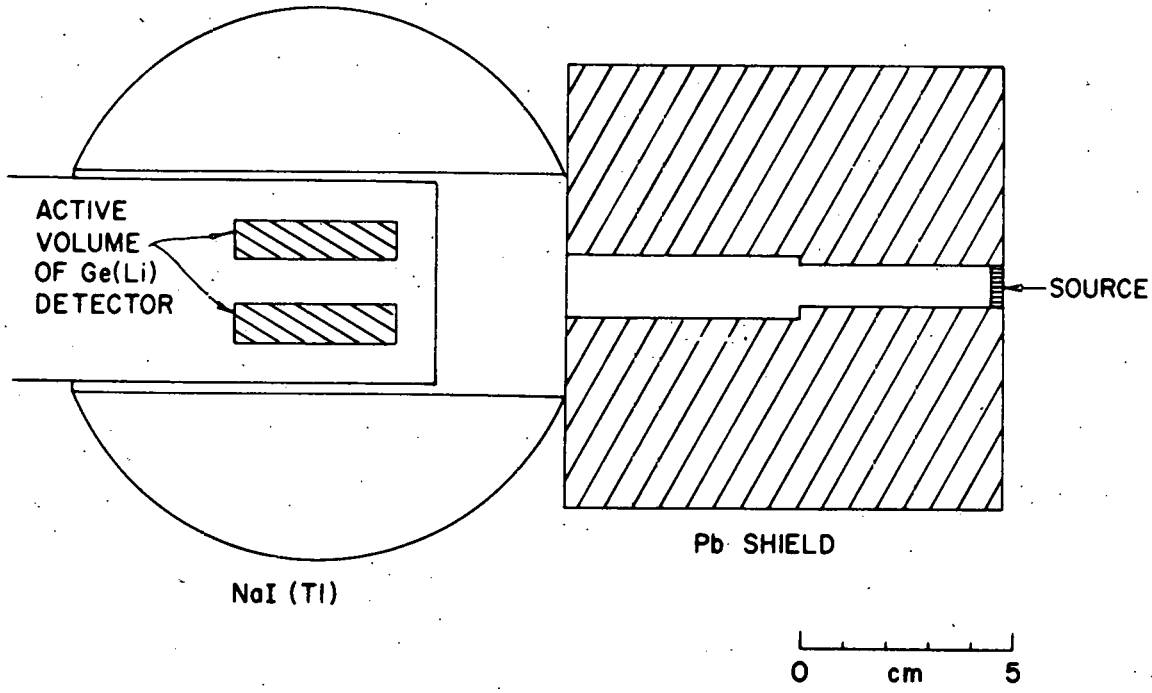

Figure 7. Cutaway side view of the three crystal spectrometer

resolution coaxial Ge(Li) detector, was mounted in a right angle cryostat. It had a drift depth of 8.5 millimeters and an active volume of 23 cubic centimeters. The recommended operating voltage was between 1200 and 1400 volts negative polarity and the total capacitance was given to be about 36 pf. The detector had a resolution of about 3 keV full width at half maximum (FWHM) at the 1332 keV photopeak of ^{60}Co. The detector-cryostat system was mounted in a 31 liter Linde dewar where it was maintained at liquid nitrogen temperature. The two identical NaI(Tl) detectors were made by the Harshaw Chemical Company upon special request. Each consisted of a thallium-activated sodium iodide crystal three inches thick and five inches in diameter with a one inch radius hemicylindrical slot machined in the front face. They were coupled by pure sodium iodide light pipes one inch thick to RCA 8055 multiplier phototubes. The crystals were hermetically sealed in 0.019 inch stainless steel cans. The phototubes were equipped with external holddown magnetic shields and low background tube base assemblies. The two NaI(Tl) detectors were mounted so that the two semi-circular slots combine to form a full circular slot in which the Ge(Li) detector was positioned. Radiation from the source was collimated through four inches of lead shielding.

C. Electronics

A block diagram of the electronics is shown in Figure 8. The pulses from the Ge(Li) detector were amplified by an Ortec Model 118A FET preamplifier which was mounted directly on the cryostat. To take off a timing signal the preamplifier's output signal is routed through an Ortec Model 260 time pickoff unit. In the main amplifier, an Ortec Model 440A selectable active filter amplifier, the pulses were properly shaped to give best system resolution (36-38). To prevent degradation of the resolution by pulse pile up caused by high counting rates, the main amplifier was connected to the Nuclear Data Series 2200 4096 channel pulse height analyzer via an Ortec Model 438 baseline restorer.

The signal from each NaI(Tl) detector was sent through an Ortec Model 113 preamplifier to a Sturrup 1411 double delay line (DDL) amplifier. The signal was then sent to a Sturrup 1435 timing single channel analyzer (SCA), which produced a standardized fast logic pulse for NaI(Tl) pulses of the selected amplitude. These pulses and the signal from the time pickoff unit in the Ge(Li) channel were fed into a Chronetics Model 157 dual AND/OR unit. The output from the AND/OR unit triggered a gating pulse for the analyzer, timed to coincide with the arrival of the delayed Ge(Li) pulse. The system had a 60 n sec resolving time. The mode of

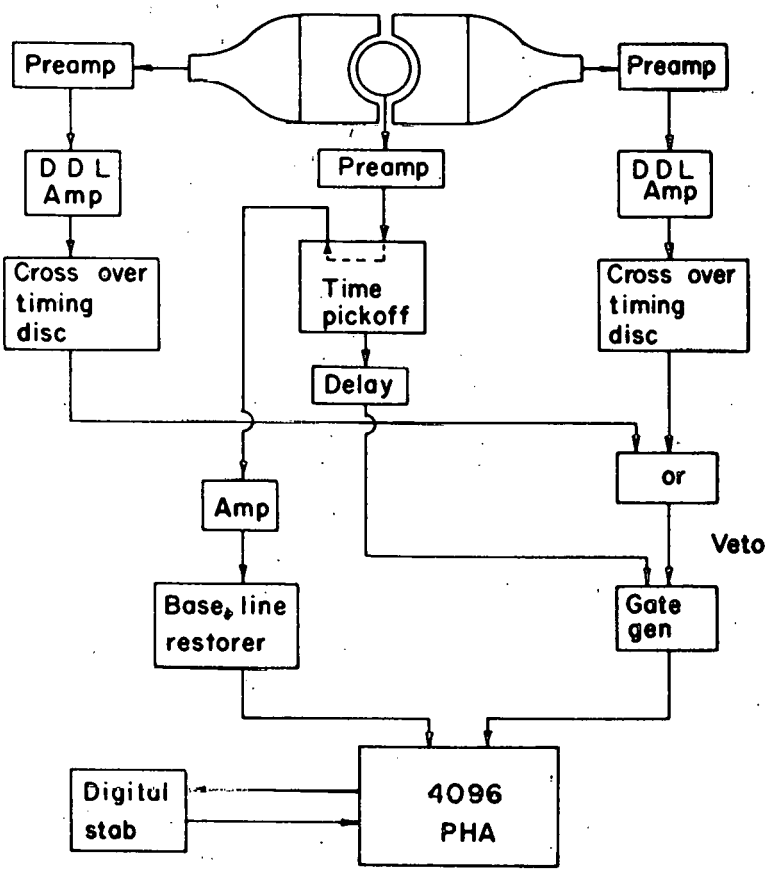

Figure 8. Block diagram of the associated electronics

operation of the three crystal spectrometer was determined by settings on the SCA and AND/OR units.

1. Pair spectrometer mode

The pair spectrometer mode requires the SCA to operate as a "window" for the 511 keV annihilation radiation. Thus only 511 keV pulses produced an output from the SCA. The AND/OR unit was set to require triple coincidences.

Figure 9 shows a gamma ray spectrum of ^{56}Co taken with the single Ge(Li) detector. Figure 10 shows the same spectrum taken in the pair spectrometer mode. The background has been substantially reduced and only double-escape peaks are present. However, the efficiency of the pair spectrometer is much less than that of a single Ge(Li) detector and requires a longer accumulation time for comparable peak counts. For example, the pair spectrum shown in Figure 10 required a twelve times longer accumulation time than the single spectrum shown in Figure 9.

2. Compton suppression mode

The Compton suppression mode requires the SCA to operate as a discriminator and the AND/OR unit is placed in the "OR" position. Whenever a pulse in the Ge(Li) detector is coincident with a pulse in either NaI(Tl) detector this is interpreted as a Compton scattering event. The analyzer is

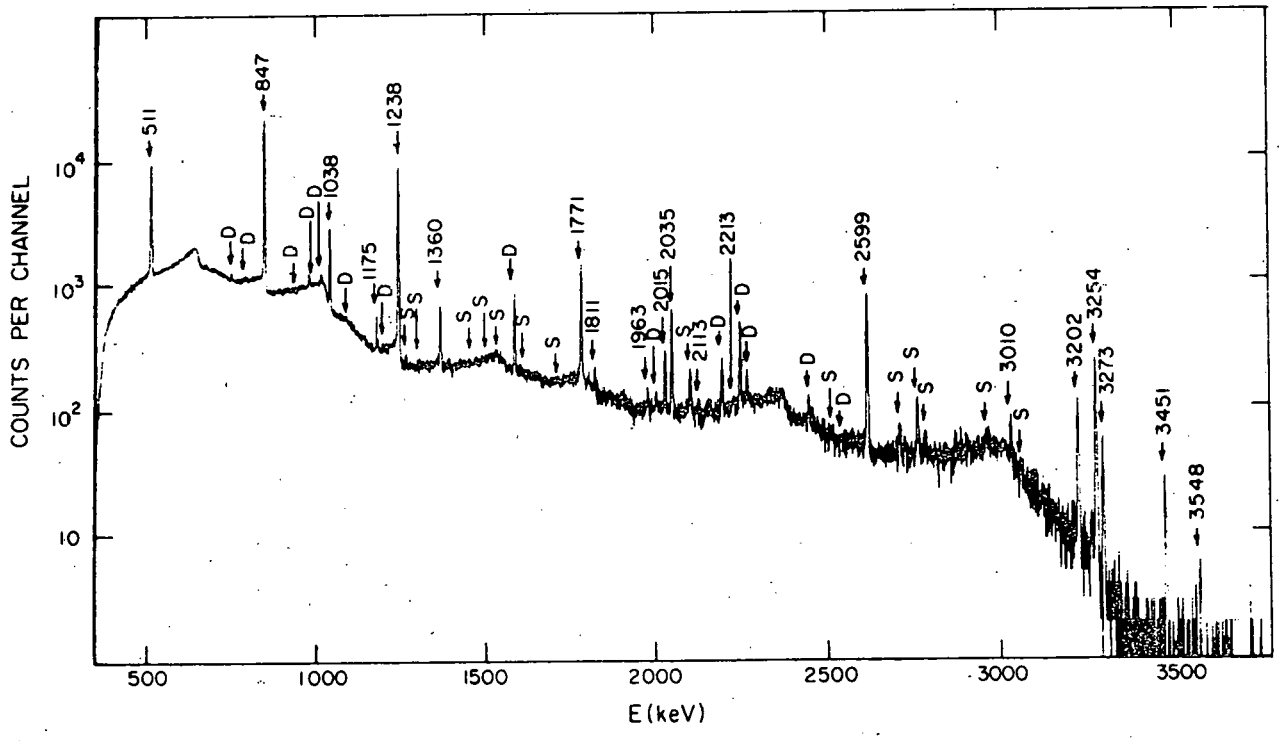

Figure 9. A 4096 channel self gated gamma ray spectrum of ^{56}Co

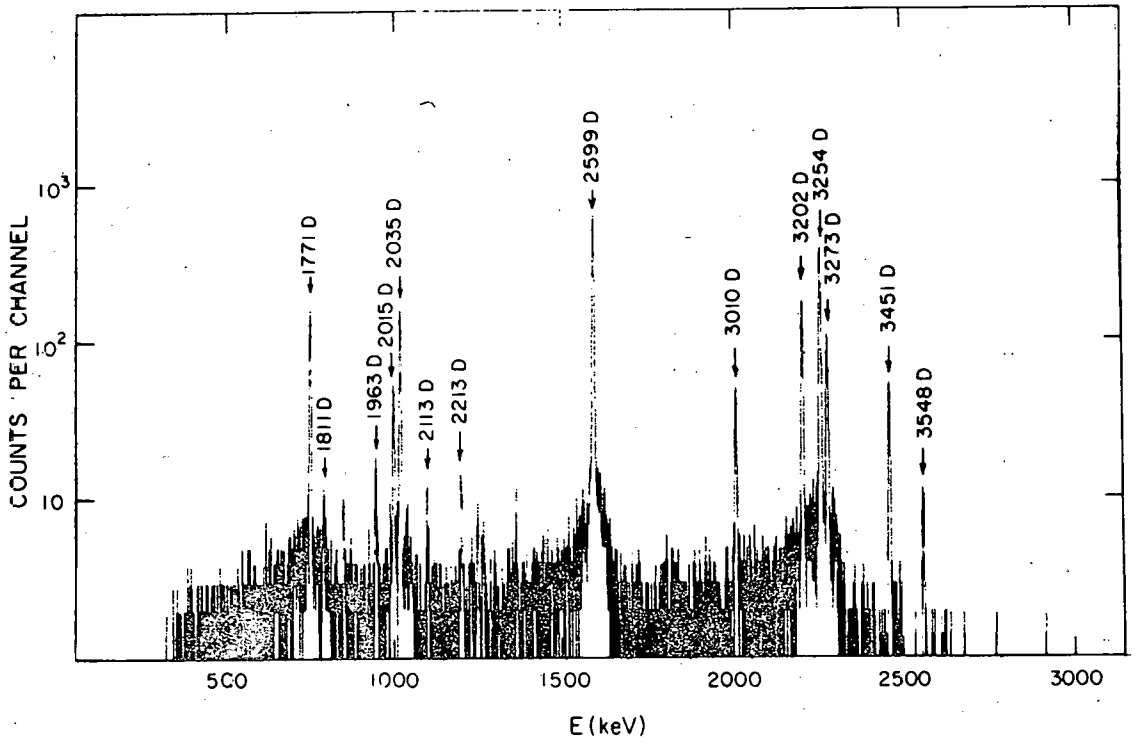

Figure 10. A 4096 channel gamma ray spectrum of ^{56}Co taken with the three crystal spectrometer in the pair spectrometer mode

gated off and the signal from the Ge(Li) detector is not recorded. A Compton suppression spectrum of ^{56}Co is shown in Figure 11.

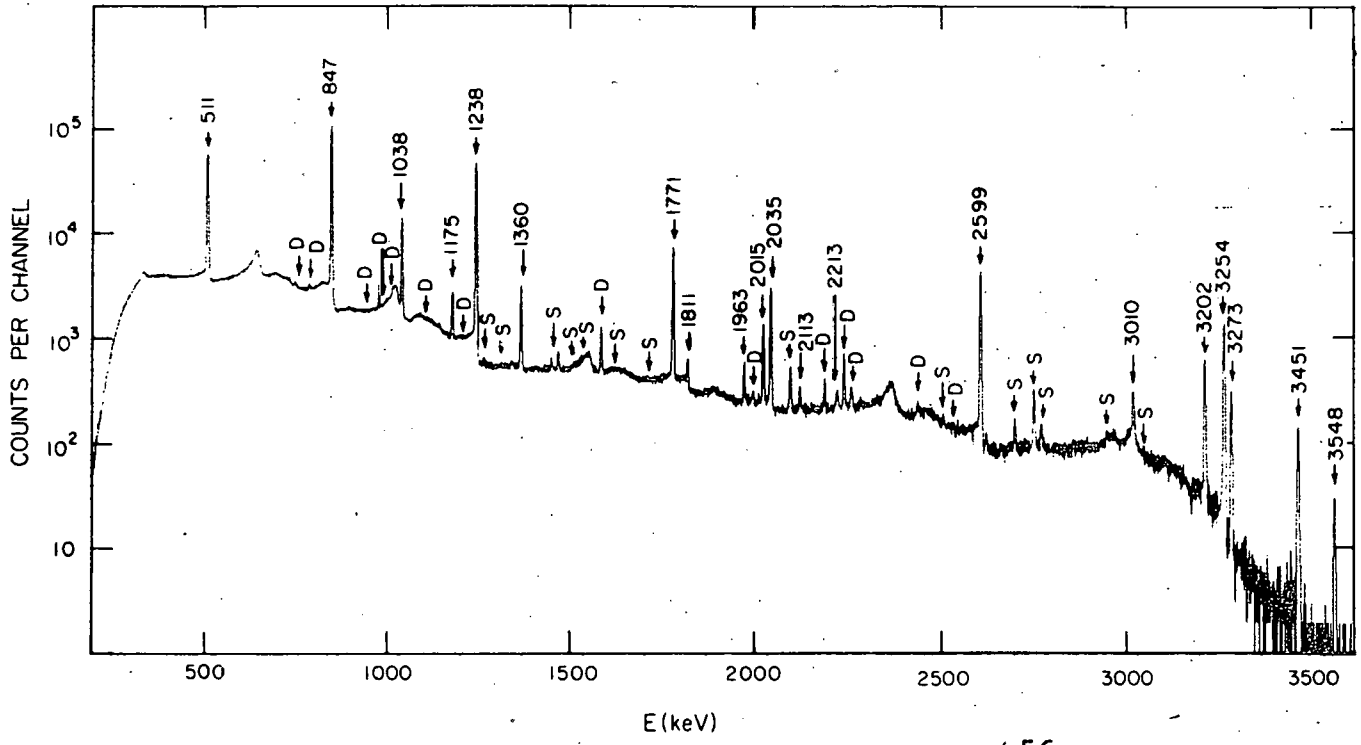

Figure 11. A 4096 channel gamma ray spectrum of ^{56}Co taken with the three crystal spectrometer in the Compton suppression mode

III. DECAY OF ^{90}Nb

The odd-odd nucleus $^{90}_{41}Nb_{49}$ undergoes β^+ and electron capture (EC) decay with $T_{1/2}$ = 14.6 hours to excited states of ^{90}Zr. The large difference between the ground state energies (6.1 MeV) and spins (for ^{90}Nb, $J^\pi = 8^+$) causes the decay to proceed through highly excited, high-spin states of ^{90}Zr (24, 28). A study of the levels in ^{90}Zr and the electromagnetic transitions from states populated in ^{90}Nb decay has been reported by many investigators (24, 29, 39, 40). The work reported in the present study is a remeasurement of the gamma ray spectrum with Compton suppression techniques to obtain intensities sufficiently accurate to determine the conversion coefficients and multipolarities of the weak transitions and thus the spins and parities of the levels involved.

A. Experiment

To reduce the Compton background from the intense high energy lines, the spectrometer was operated in the Compton suppression mode explained previously in Part II. This system reduced the Compton plateau of the 2319 and 2186 keV lines by a factor of four from that obtained with the Ge(Li) detector alone.

Sources were obtained from the reaction ^{92}Mo(γ,np)^{90}Nb

and $^{92}Mo(\gamma,2n)^{90}M\rightarrow^{90}Nb$ by placing a 1.5 gram sample of molybdenum metal (16% ^{92}Mo) in a bremsstrahlung beam from the ISU 70 MeV electron synchrotron. After a three hour bombardment, a series of gamma ray spectra were recorded during a 50 hour counting period. Digital stabilization was used to eliminate peak broadening due to gain shifts. The combined spectrum is shown in Figure 12. These data were analyzed by a computer program which fits a Gaussian line shape to each peak after subtracting a smoothed background (41). Examples of the computer fits to strong and weak peaks are shown in Figure 13.

Most of the gamma rays from 15 hour ^{90}Nb decay could easily be distinguished by decay rate from other Mo and Nb activities. This decay was not a simple exponential, since ^{90}Nb was continually being produced in the decay of 5.7 hour ^{90}Mo. Therefore the ratio of photopeak areas to that of the 2319 keV gamma ray was used to check the assignment to ^{90}Nb decay. Figure 14 in a plot of this ratio for all the peaks investigated except for the 518 keV transition, which was obscured by the intense annihilation radiation. The area of this peak was estimated from the combined spectrum. This gamma ray was observed by Cooper et al. (28) in a study of ^{90}Mo decay and assigned to that activity but not placed in the decay scheme. In their investigation of conversion electrons from chemically separated ^{90}Mo and ^{90}Nb sources,

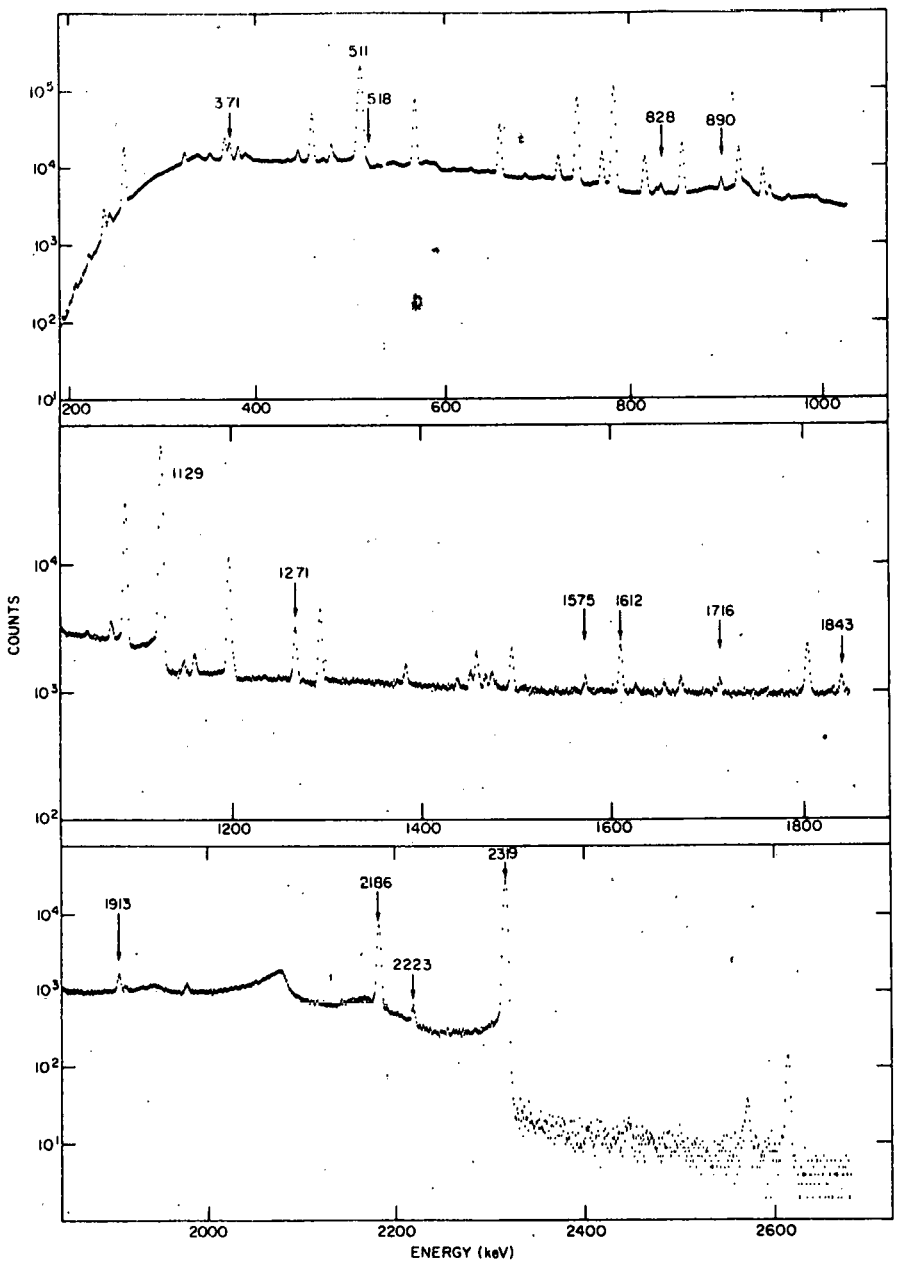

Figure 12. A 4096 channel gamma ray spectrum of irradiated Mo recorded with Compton suppression. Lines above 300 keV assigned to ^{90}Nb decay are labelled with their energies

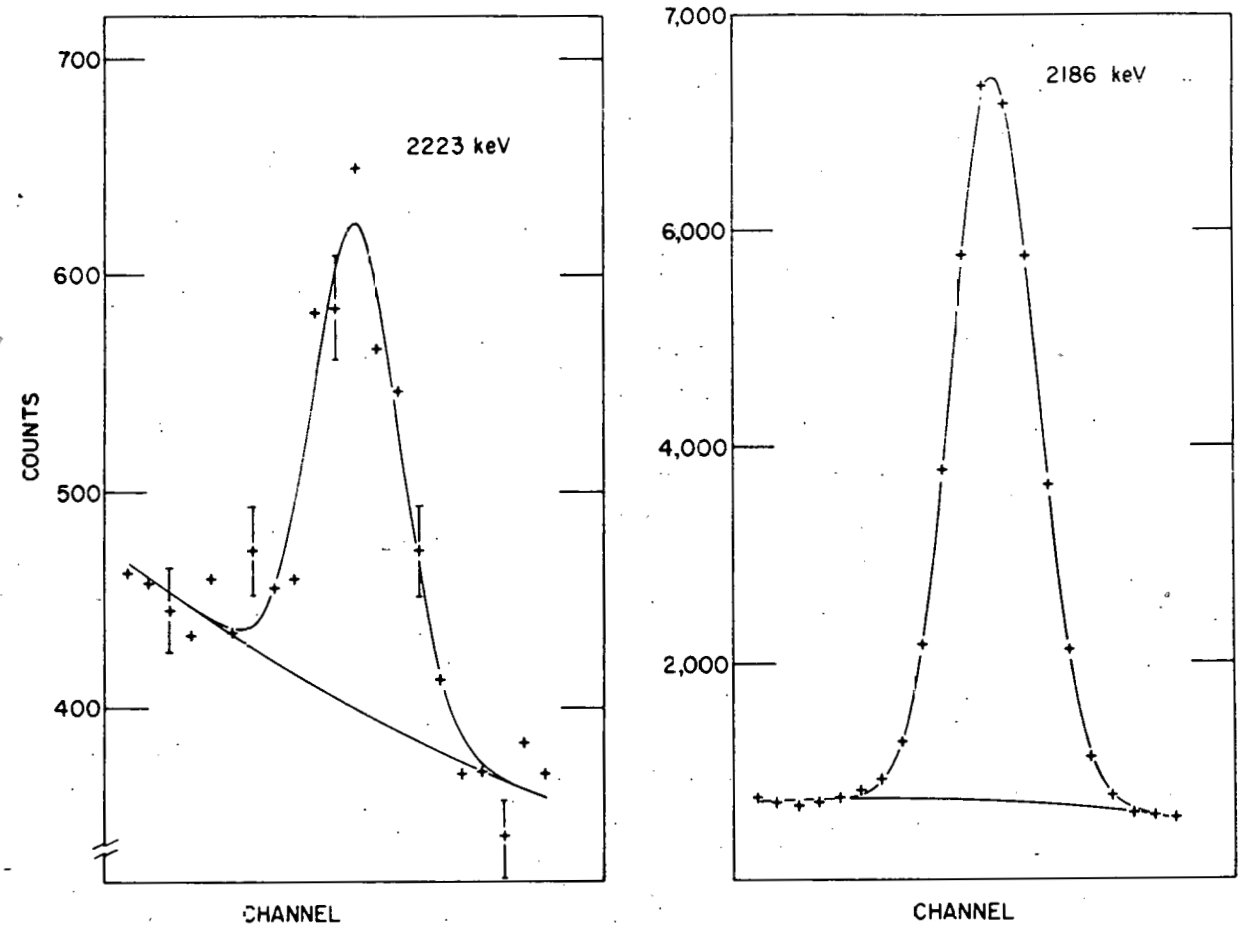

Figure 13. Sample computer fits to weak and strong peaks

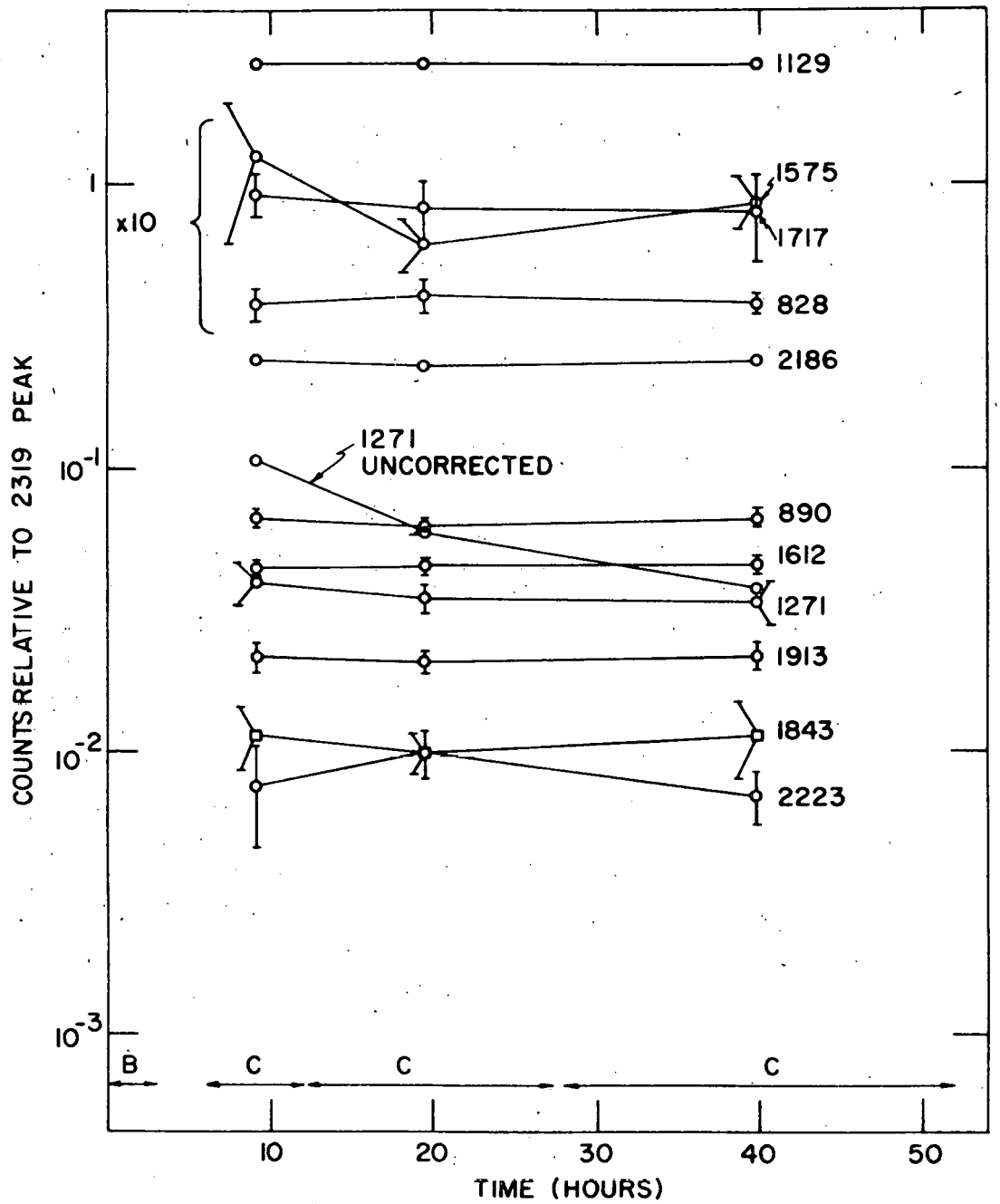

Figure 14. Photopeaks area ratios used to confirm ^{90}Nb assignment. Bombardment and counting periods are indicated with B and C

Pettersson et al. have assigned this transition to ^{90}Nb decay (24, 42)

Another case which required special treatment was the photopeak at 1271 keV, for ^{90}Mo decay also has a transition at 1271.3 keV (28). The contribution from this gamma ray was calculated from the area of the photopeak of the 942 keV ^{90}Mo gamma ray, the relative intensity given in reference 28, and the detector's efficiency function (Figure 15), then subtracted from the total peak area. The success of this correction can be seen in Figure 14.

The spectrometer was calibrated with a ^{56}Co source which has many gamma rays with precisely known energies and intensities in the range of interest of this experiment (43). Relative photopeak detection efficiency as a function of gamma ray energies is shown in Figure 15. Since the source had to be separated from the Ge(Li) detector by several centimeters to allow for shielding the NaI(Tl) scintillators from the direct radiation the absolute efficiency was less than in conventional Ge(Li) singles spectroscopy.

Energies of the gamma rays were determined with a combined source technique. First a ^{56}Co spectrum was recorded and analyzed with the computer program described previously. The deviation from linearity of the gamma-ray energy as a function of peak channel number was less than 0.2 keV between 800 and 2500 keV (see Figure 16). Next a spectrum of a

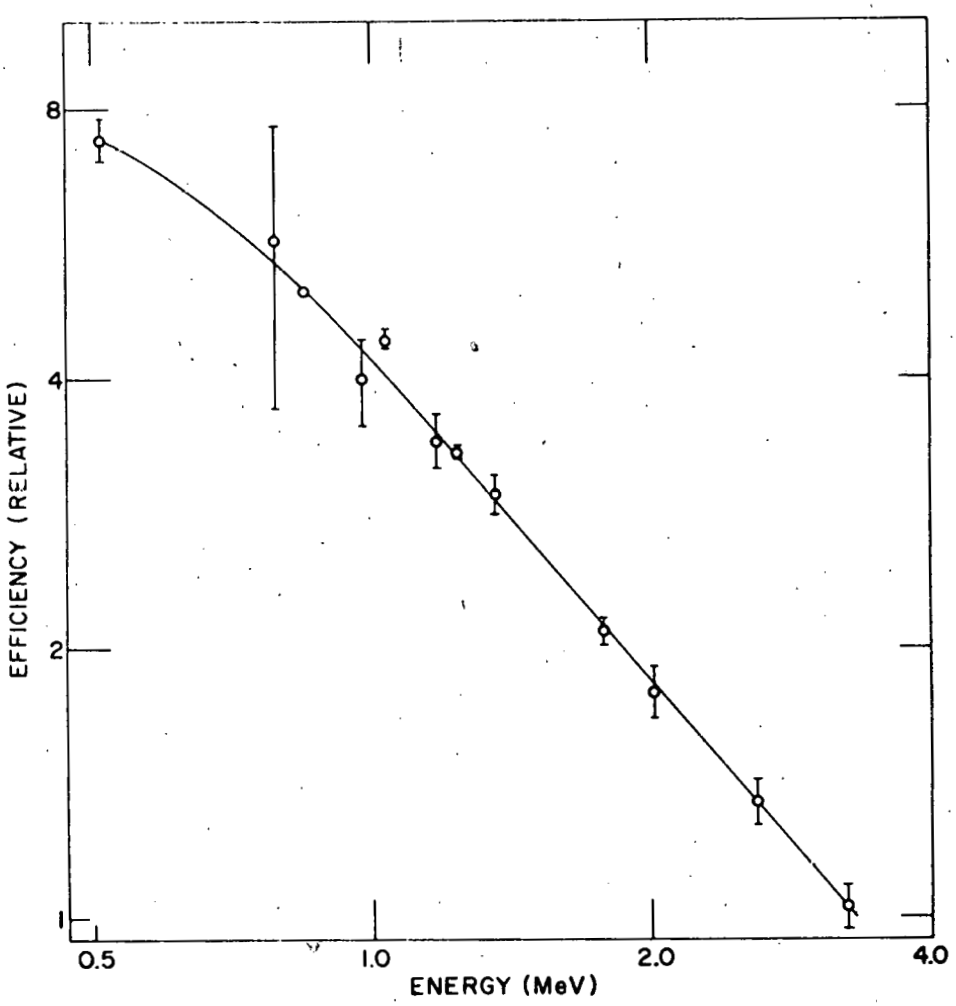

Figure 15. Relative efficiency of the Compton suppression spectrometer determined with ^{56}Co sources

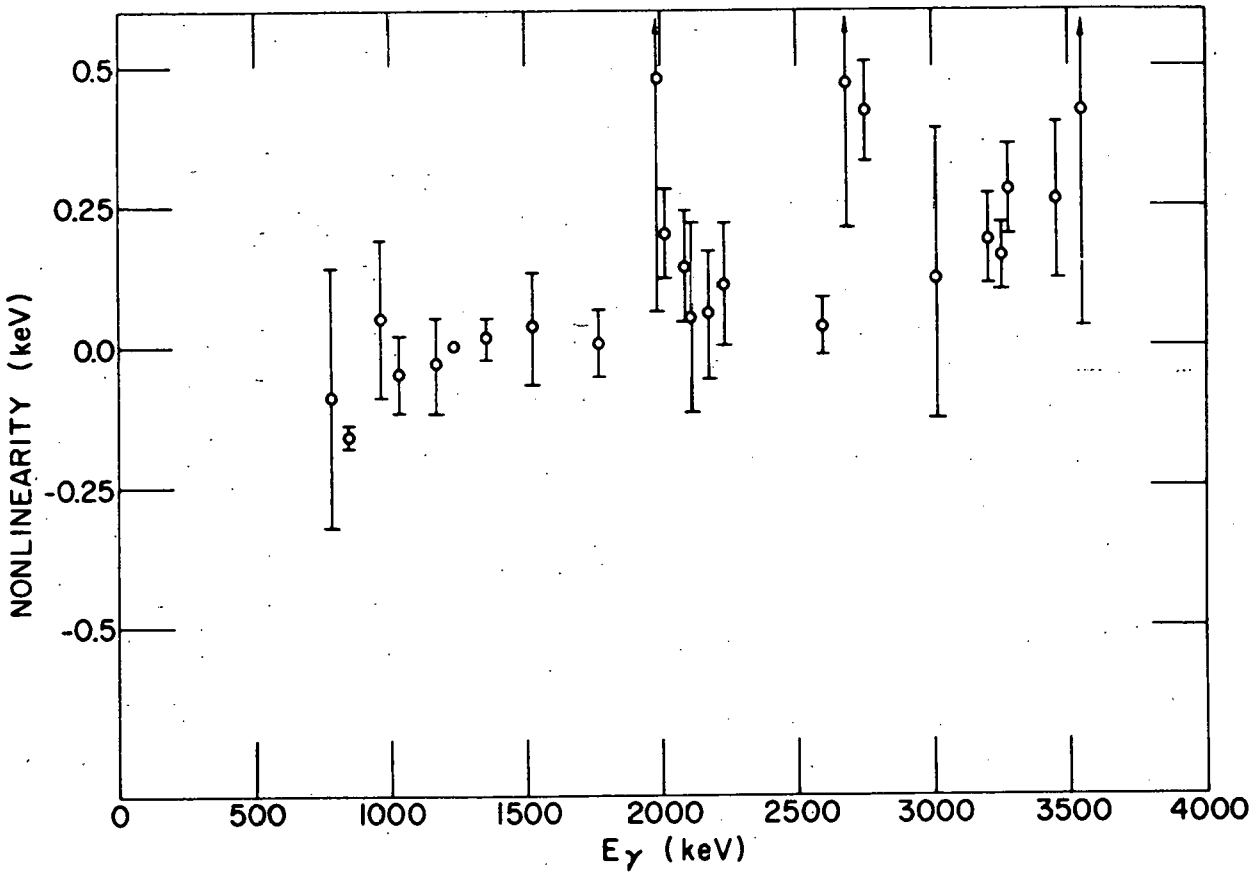

Figure 16. Deviation from linearity measured with a ^{56}Co source

combined ^{56}Co and irradiated Mo source was recorded, the ^{56}Co gamma rays providing an internal calibration used to determine the energies of the strong Mo peaks. The non-linearity data of Figure 16 were used to extrapolate between calibration peaks. Then the ^{56}Co source was removed and a third spectrum accumulated. Energies of the weak lines were measured from these data, with the strong lines serving as calibration points. A conservative error estimate is $\pm$ 0.2 keV for most of the ^{90}Nb gamma rays studied.

B. Results

Table 1 summarizes the numerical results of this experiment. Transition energies determined with conversion electron spectroscopy techniques by Pettersson et al. (24) are in excellent agreement with the gamma ray energies measured in the present work. Gamma ray absolute intensities were calculated from the measured relative intensities by setting the sum of the 2186 and 2319 keV ground state transitions equal to 100% (see Figure 18). A 5% systematic uncertainty in the relative efficiency function for the spectrometer was combined with the statistical errors in photopeak areas to determine errors for the intensities. Conversion coefficients were calculated from the K-conversion electron intensities reported in reference (24).

Table 1. Measured gamma-ray intensities and deduced K-conversion coefficients and multipolarities

Transition energy (keV)		Gamma intensity (% ^{90}Nb decays)		$1_K \times 10^4$ [a]	$\alpha_K \times 10^4$		Multipolarity
Present work	Pettersson et al.	Present work	Pettersson et al.	Pettersson et al.	Present work	Pettersson et al.	
518(1)	518.2(2)	0.5(3)		14.2(9)	28(17)		M1,E2[b])
827.8(4)	827.7(4)	0.90(7)	<2.0	3.76(32)	4.2(5)		E1
890.6(2)	890.54(35)	1.73(12)	<2.0	13.1(7)	7.57(6)	>5.8	M1,E2[b])
1129.1(2)	1129.1(3)	92.0(5)	89.0(4)	186(6)	2.02(12)	2.10(24)	E1
1270.6(2)	1270.5(5)	1.45(13)	0.9(4)	8.0(6)	5.6(7)	9(4)	E3
1574.8(2)	1575.0(7)	0.47(7)		1.17(28)	2.5(7)		M1,E2
1611.8(2)	1612.1(4)	2.4(2)	4.0(15)	5.7(4)	2.38(23)	1.4(8)	M1,E2
1716.2(4)	1716.6(12)	0.52(5)		1.11(37)	2.1(7)		M1,E2[b])
1843.3(2)	1842.9(9)	0.75(15)		1.18(15)	1.57(37)		M1,E2
1913.3(2)	1913.5(9)	1.30(23)		1.92(20)	1.48(30)		M1,E2
2186.4(2)	2186.2(4)	18.0(9)	17.9(27)	22.2(13)	1.23(9)	1.29(26)	E2[a])
2222.5(4)	2223.3(10)	0.64(9)	0.70(35)	0.63(19)	1.0(3)	0.9(5)	E1[b]),M1, E2
2319.2(2)	2318.6(4)	82.0(4)	82.0(10)	329(7)	4.0(2)	4.2(7)	E5[a])

(Errors in the least significant digits are given in parentheses)

[a]Absolute intensities were determined by equating conversion coefficients for the E2 2186 and E5 2319 transitions to the theoretical values of ref.(44).

[b]Favored in decay scheme.

In Figure 17 the K-conversion coefficients listed in Table 1 are compared with theoretical values computed by Sliv and Band (44). (Note that the K-conversion electron intensities given in reference 24 were normalized by matching the conversion coefficients for the pure E2 and E5 ground state transitions to the theoretical values.) The order of magnitude of K-conversion coefficients does not vary rapidly with multipolarity at these energies. However, the data are sufficiently accurate to identify most of the transitions as E2 or M1.

A decay scheme for ^{90}Nb is proposed in Figure 18. Only those levels in ^{90}Zr involved in the observed electromagnetic transitions are shown. The 133, 141, and 371 keV transitions (24), which were not restudied in the present experiment are included for completeness. Placement of the transitions is the same as in reference (24). Total β^+ and EC feeding to each level was determined from the difference between gamma ray intensities into and out of the state. Log ft values were calculated from these branchings, the quantities Q = 6.111 MeV and $T_{1/2}$ = 14.6 hour, the theoretical EC/β^+ ratios and β-decay nomograms in Appendix IV of Table of Isotopes (45).

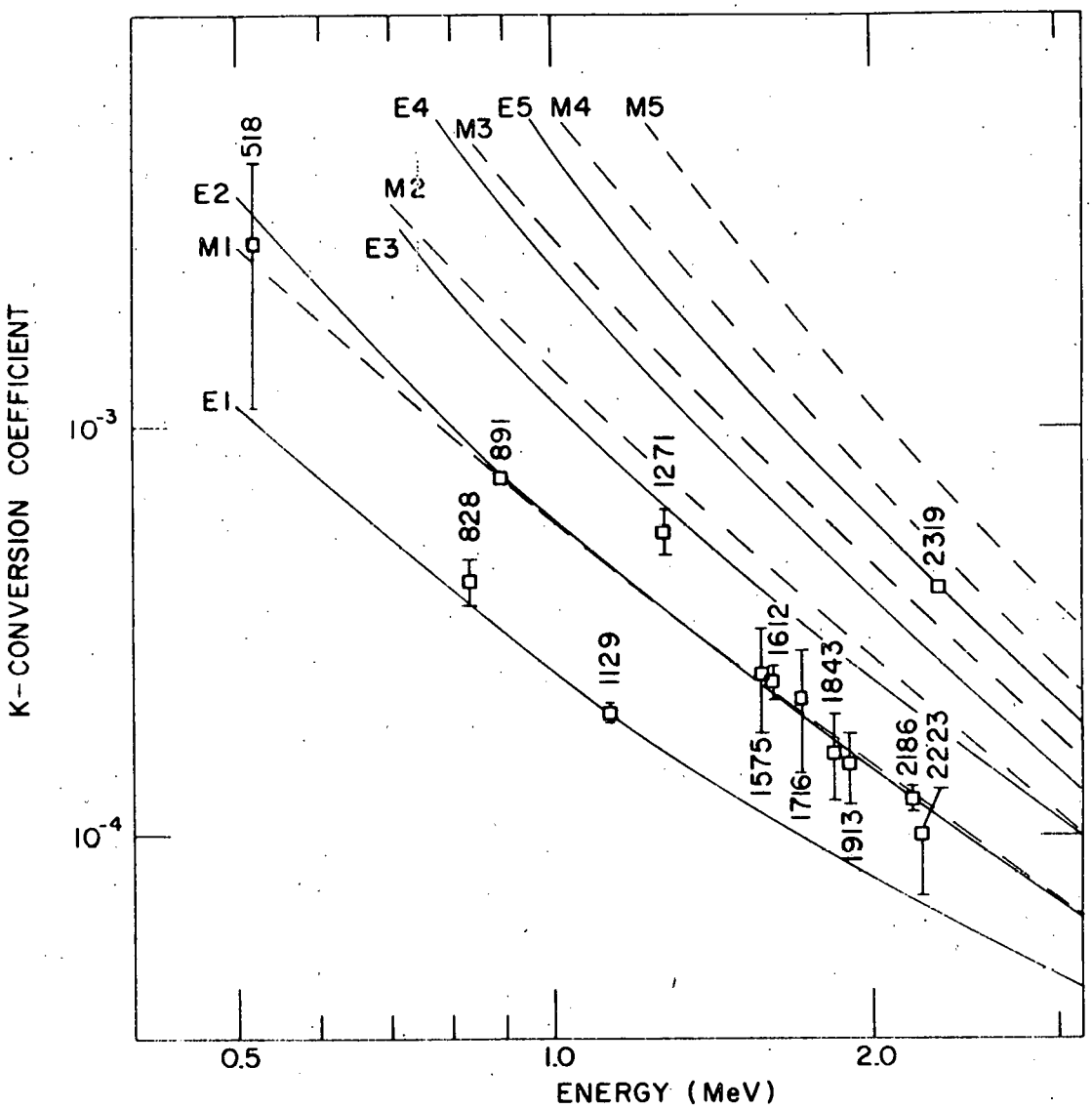

Figure 17. Conversion coefficients calculated from data summarized in Table 1. Lines are the theoretical values of Sliv and Band

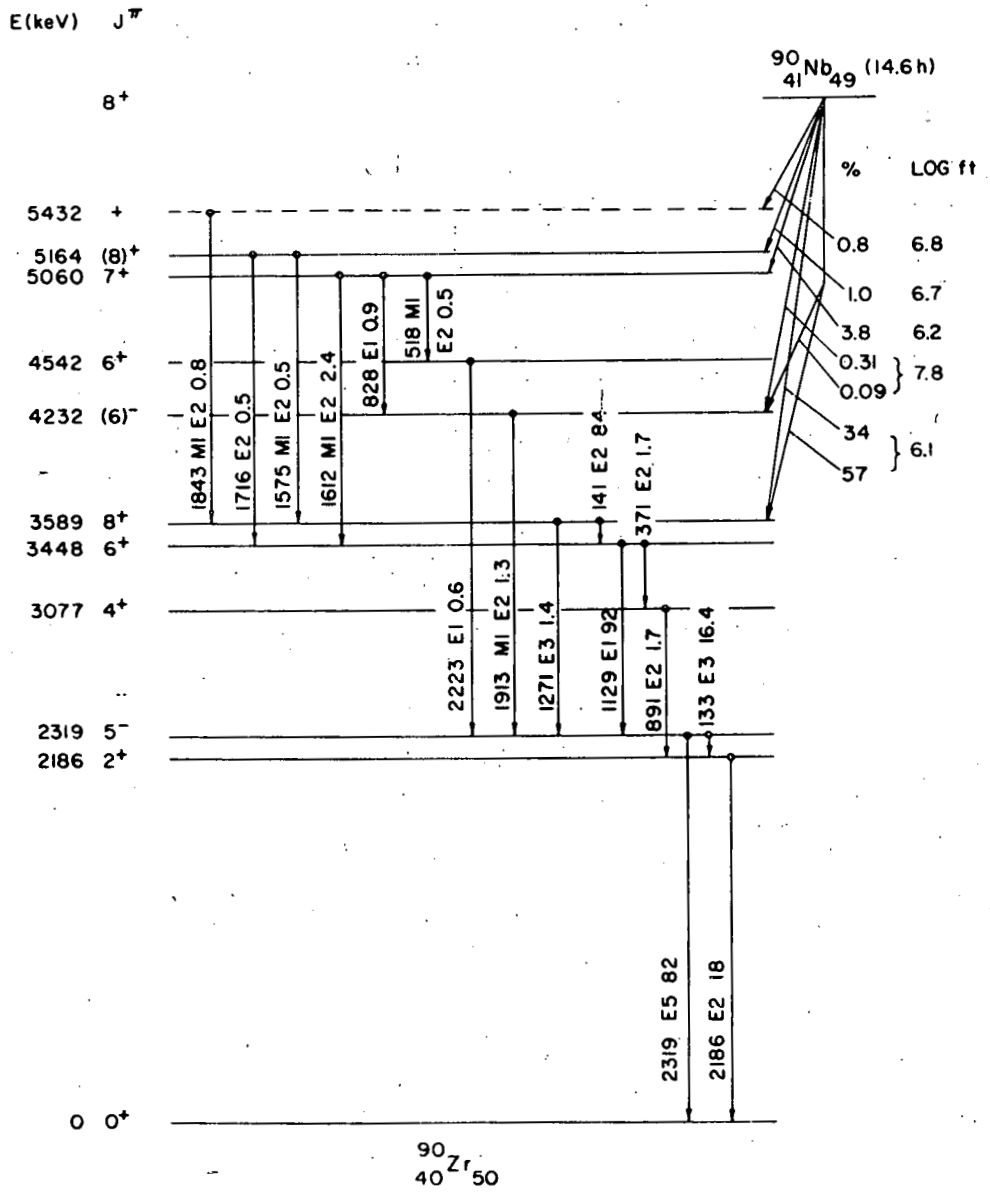

Figure 18. Decay scheme for ^{90}Nb proposed from this investigation. Transitions between levels in ^{90}Zr are labelled with energy, probable multipolarity and intensity

IV. THEORETICAL CALCULATIONS

In 1955 K. W. Ford (13) suggested that the levels of $^{90}_{40}Zr_{50}$ below 3600 keV could be explained by assuming the 38 protons which close the $1f\frac{5}{2}$ subshell and the 50 neutrons which close the $1g\frac{9}{2}$ "magic number" shell form an inert core about which the remaining 2 protons couple to produce the low lying levels. In this model the basic configurations of these protons are $(2p\frac{1}{2})^2$, $(1g\frac{9}{2})(2p\frac{1}{2})$ and $(1g\frac{9}{2})^2$. The $(2p\frac{1}{2})^2$ and the $(1g\frac{9}{2})^2$ configurations are mixed in the first excited 0^+ level and the ground 0^+ level. The $(1g\frac{9}{2})^2$ configuration also gives the 2^+, 4^+, 6^+, and 8^+ levels. The $(1g\frac{9}{2})(2p\frac{1}{2})$ configuration is responsible for the 5^- and 4^- levels. However if the wave functions for the 6^+ and 5^- states were pure $(1g\frac{9}{2})^2$ and $(1g\frac{9}{2})(2p\frac{1}{2})$ respectively, there could be no E1 transition between these levels. The E1 operator can change the orbital angular momentum by only one unit; a $g\frac{9}{2} \rightarrow p\frac{1}{2}$ transition would require emission of an M4 or E5 photon. The experimental facts that a strong E1 transition goes between these two states and that the favored $6^+ \rightarrow 4^+$ E2 transition competes very weakly (see Figure 18) contradicts the simple shell model theory of this nucleus. Therefore at least one of the states (6^+ and 5^-) is more complicated than previously proposed. The question to be answered is the following. How much must the given configura-

tions be altered in order to give this strong E1 transition between the 6^+ and 5^- levels? If a large amount of configuration mixing is necessary this will lead to serious doubt in using the simple shell model interpretation for this nucleus. This is an important test, since ^{90}Zr is in the region where the shell model interpretation is expected to work best, near closed shells.

As a first approximation the 5^- state is assumed to have some $(1g\frac{9}{2})(1h\frac{11}{2})$ configuration mixed in it since $(1h\frac{11}{2})$ is the first odd parity level available to the two extra-core protons (see Figure 1). For brevity the $(1g\frac{9}{2})$, $(2p\frac{1}{2})$, and $(1h\frac{11}{2})$ configurations will be written simply as $(g\frac{9}{2})$, $(p\frac{1}{2})$ and $(h\frac{11}{2})$. Thus the 5^- state wavefunction is written as:

$$(1) \quad |5^-) = a[(g\tfrac{9}{2})(p\tfrac{1}{2})]_5 + b[(g\tfrac{9}{2})(h\tfrac{11}{2})]_5 \ .$$

The 6^+ state wavefunction is taken to be that suggested by the simple shell model in this case, namely:

$$(2) \quad |6^+) = [(g\tfrac{9}{2})^2]_6 = [(g\tfrac{9}{2})(g\tfrac{9}{2})]_6 \ .$$

In a similar manner the 4^+ state wavefunction is written as:

$$(3) \quad |4^+) = [(g\tfrac{9}{2})^2]_4 = [(g\tfrac{9}{2})(g\tfrac{9}{2})]_4 \ .$$

The subscript outside the brackets is the total angular momentum to which the two angular momenta are coupled. The objective of this calculation is to find the value of b in Equation (1). The program for determining b is to compute the ratio of $(6^+ \rightarrow 5^-)$ to $(6^+ \rightarrow 4^-)$ transition probabilities as a function of b and to set the result equal to the ratio of the experimentally observed intensities:

$$(4) \quad \frac{I_\gamma(6^+ \rightarrow 5^-)}{I_\gamma(6^+ \rightarrow 4^+)} = \frac{T(6^+ \rightarrow 5^-)}{T(6^+ \rightarrow 4^+)}$$

where the intensities are denoted by I and the transition probabilities by T. The physically meaningful transition probability is given by (46):

$$(5) \quad T_{fi} = \frac{8\pi}{[(2J+1)!!]^2} \left(\frac{J+1}{J\hbar}\right) k^{2J+1} \left|(f|O_{op}|i)\right|^2$$

where

$$(6) \quad k = \frac{E_\gamma}{\hbar c} .$$

J is the multipolarity of the transition and i and f denote initial and final states respectively. Therefore the following matrix elements must be evaluated:

$$\left|(5^-|(E1)_{op}|6^+)\right|^2$$

and

$$\left|(4^+|(E2)_{op}|6^+)\right|^2 .$$

Normalization of the $|6^+)$ wavefunction is not required since the normalization factor will cancel out in the ratio of transition probabilities. However it is important that the $|4^+)$ and $|5^-)$ wavefunctions are normalized. First consider the $|4^+)$ wavefunction:

$$(7)\quad |4^+) = N \frac{1}{2} \sum_{kl} (-1)^{\frac{9}{2}-\frac{9}{2}-m} \hat{4} \begin{pmatrix} \frac{9}{2} & \frac{9}{2} & 4 \\ k & 1 & -m \end{pmatrix} \times$$

$$\times \{\phi_{\frac{9}{2}k}(1)\ \phi_{\frac{9}{2}l}(2) - \phi_{\frac{9}{2}k}(2)\ \phi_{\frac{9}{2}l}(1)\} .$$

The wavefunction is normalized by the constant N. It is written in antisymmetric form since it applies to identical particles. The wavefunction in Equation (7) above is formed by taking a linear combination of products of wavefunctions of the individual particles. The coefficients in the expansion are called 3-j symbols, the properties of which are fully discussed in reference (47). The individual particle wavefunctions are taken to be those predicted by the simple shell model (12). The symbol $\hat{p}$ denotes $(2p+1)^{1/2}$ where p is some number. Carrying out the multiplication in Equation (7) gives:

$$(8)\quad |4^+) = N \frac{1}{2} \sum_{kl} (-1)^m \hat{4} \begin{pmatrix} \frac{9}{2} & \frac{9}{2} & 4 \\ k & 1 & -m \end{pmatrix} \times \phi_{\frac{9}{2}k}(1)\ \phi_{\frac{9}{2}l}(2)$$

$$- N \frac{1}{2} \sum_{kl} (-1)^m \hat{4} \begin{pmatrix} \frac{9}{2} & \frac{9}{2} & 4 \\ k & 1 & -m \end{pmatrix} \phi_{\frac{9}{2}k}(2)\ \phi_{\frac{9}{2}l}(1)$$

Equation (8) can be simplified by interchanging the summation indices k and l in the second term. This will give a 3-j symbol of the form

$$\begin{pmatrix} \frac{9}{2} & \frac{9}{2} & 4 \\ l & k & -m \end{pmatrix}$$

which can be written using the symmetry properties of the 3-j symbol as

$$(-1)^{\frac{9}{2}+\frac{9}{2}+4}\begin{pmatrix} \frac{9}{2} & \frac{9}{2} & 4 \\ k & l & -m \end{pmatrix} = -\begin{pmatrix} \frac{9}{2} & \frac{9}{2} & 4 \\ k & l & -m \end{pmatrix} .$$

With this substitution Equation (8) becomes:

$$(9)\quad |4^+) = N\frac{1}{2}\sum_{kl}(-1)^m \hat{4}\begin{pmatrix} \frac{9}{2} & \frac{9}{2} & 4 \\ k & l & -m \end{pmatrix}\phi_{\frac{9}{2}k}(1)\,\phi_{\frac{9}{2}l}(2) + N\frac{1}{2}\sum_{kl}(-1)^m \hat{4}\begin{pmatrix} \frac{9}{2} & \frac{9}{2} & 4 \\ k & l & -m \end{pmatrix}\phi_{\frac{9}{2}l}(2)\,\phi_{\frac{9}{2}k}(1) .$$

Inspection of Equation (9) shows that it is the sum of two identical terms which can be combined. Thus:

$$(10)\quad |4^+) = N\sum_{kl}(-1)^m \hat{4}\begin{pmatrix} \frac{9}{2} & \frac{9}{2} & 4 \\ k & l & -m \end{pmatrix}\phi_{\frac{9}{2}k}(1)\,\phi_{\frac{9}{2}l}(2) .$$

The normalization factor N is determined by requiring $(4^+|4^+) = 1$ where it has been assumed that the single particle

wavefunctions are normalized. Using Equation (10) for $|4^+)$ the normalization condition becomes:

$$(11)\quad (4^+|4^+) = N^2 \sum_{\substack{k\,l\\ k'l'}} \hat{4}\,\hat{4} \begin{pmatrix} \frac{9}{2} & \frac{9}{2} & 4 \\ k & 1 & -m \end{pmatrix} \begin{pmatrix} \frac{9}{2} & \frac{9}{2} & 4 \\ k' & 1' & -m' \end{pmatrix} \times$$

$$\times (-1)^{m+m'} \left(\phi_{\frac{9}{2}k}(1) \middle| \phi_{\frac{9}{2}k'}(1)\right) \left(\phi_{\frac{9}{2}l}(2) \middle| \phi_{\frac{9}{2}l'}(2)\right)$$

$$= N^2 \sum_{\substack{k\,l\\ k'l'}} (-1)^{m+m'} \hat{4}\,\hat{4} \begin{pmatrix} \frac{9}{2} & \frac{9}{2} & 4 \\ k & 1 & -m \end{pmatrix} \begin{pmatrix} \frac{9}{2} & \frac{9}{2} & 4 \\ k' & 1' & -m' \end{pmatrix} \times$$

$$\times \quad \delta_{kk'}\,\delta_{ll'} = N^2 (-1)^{m+m'} \sum_{kl} \hat{4}\,\hat{4} \times$$

$$\times \begin{pmatrix} \frac{9}{2} & \frac{9}{2} & 4 \\ k & 1 & -m \end{pmatrix} \begin{pmatrix} \frac{9}{2} & \frac{9}{2} & 4 \\ k & 1 & -m' \end{pmatrix} = N^2 (-1)^{m+m'} \delta_{mm'}$$

$$= N^2 = 1$$

Thus,

$N = 1$ for the $|4^+)$ wavefunction. The complete normalized, antisymmetrized $|4^+)$ wavefunction is given by

$$(12)\quad |4^+) = \sum_{kl} (-1)^m \hat{4} \begin{pmatrix} \frac{9}{2} & \frac{9}{2} & 4 \\ k & 1 & -m \end{pmatrix} \phi_{\frac{9}{2}k}(1)\ \phi_{\frac{9}{2}l}(2)$$

The normalization of the $|4^+)$ wavefunction was done in detail to demonstrate the method used. Using this same method of normalization and a great deal more work the $|5^-)$ wavefunction can be written in its complete normalized,

antisymmetrized form as follows:

$$(13)\quad |5^-) = a\frac{1}{\sqrt{2}}\sum_{np}(-1)^{\frac{1}{2}-\frac{9}{2}-u}\hat{5}\begin{pmatrix}\frac{9}{2} & \frac{1}{2} & 5\\ n & p & -u\end{pmatrix}\times$$

$$\{\phi_{\frac{9}{2}n}(1)\,\phi_{\frac{1}{2}p}(2) - \phi_{\frac{9}{2}n}(2)\,\phi_{\frac{1}{2}p}(1)\}$$

$$+\ b\frac{1}{\sqrt{2}}\sum_{ts}(-1)^{\frac{11}{2}-\frac{9}{2}-u}\times$$

$$\hat{5}\begin{pmatrix}\frac{9}{2} & \frac{11}{2} & 5\\ t & s & -u\end{pmatrix}\{\phi_{\frac{9}{2}t}(1)\,\phi_{\frac{11}{2}s}(2) - \phi_{\frac{9}{2}t}(2)\,\phi_{\frac{11}{2}s}(1)\}$$

where Equation (13) is subject to the restriction

$$(14)\quad |a|^2 + |b|^2 = 1.$$

The $|6^+)$ wavefunction is written as

$$(15)\quad |6^+) = \sum_{wv}(-1)^z\,\hat{6}\begin{pmatrix}\frac{9}{2} & \frac{9}{2} & 6\\ w & v & -z\end{pmatrix}\phi_{\frac{9}{2}w}(1)\,\phi_{\frac{9}{2}v}(2)\quad .$$

Now as explained previously the $(6^+\to 5^-)$ transition in ^{90}Zr is known to go by E1, but the E1 operator cannot connect a $g\frac{9}{2}$ state with a $p\frac{1}{2}$ state. Therefore when the matrix element between the $|5^-)$ and $|6^+)$ states are taken, only the second term in the expression for the $|5^-)$ wave-

function enters into the calculation.

$$(16)\quad (5^-|(El)_{op}|6^+) = \frac{1}{\sqrt{2}}\, b \sum_{ts} (-1)^{1-u}\, \hat{5} \begin{pmatrix} \frac{9}{2} & \frac{11}{2} & 5 \\ t & s & -u \end{pmatrix} \times$$

$$\times \{\phi^+_{\frac{9}{2}t}(1)\ \phi^+_{\frac{11}{2}s}(2)$$

$$- \phi^+_{\frac{9}{2}t}(2)\ \phi^+_{\frac{11}{2}s}(1)\} \Big| \sum_{i=1}^{2} e_i\, r_i\, Y^*_{1M}(\hat{r}_i) \Big| \times$$

$$\times \sum_{wv} (-1)^z\, \hat{6} \begin{pmatrix} \frac{9}{2} & \frac{9}{2} & 6 \\ w & v & -z \end{pmatrix} \phi_{\frac{9}{2}w}(1)\ \phi_{\frac{9}{2}v}(2)\ .$$

Equation (16) can be simplified by expanding the El operator and applying the orthogonality condition to the single particle wavefunctions. This leads to the following expression:

$$(17)\quad (5^-|(El)_{op}|6^+) = \frac{1}{\sqrt{2}}\, b \sum_{\substack{ts \\ wv}} (-1)^{1-u}\, (-1)^z \times$$

$$\times \begin{pmatrix} \frac{9}{2} & \frac{11}{2} & 5 \\ t & s & -u \end{pmatrix} \begin{pmatrix} \frac{9}{2} & \frac{9}{2} & 6 \\ w & v & -z \end{pmatrix} \hat{6}\ \hat{5}\ \times$$

$$\times \{\delta_{tw} (\phi_{\frac{11}{2}s}(2)|e\, r_2\, Y^*_{1M}(\hat{r}_2)|\phi_{\frac{9}{2}v}(2))$$

$$- \delta_{tv}\ (\phi_{\frac{11}{2}s}(1)|e\, r_1\, Y^*_{1M}(\hat{r}_1)|\phi_{\frac{9}{2}w}(1))\}.$$

Multiplying out Equation (17) results in two terms as follows:

$$(18)\quad (5^-|(E1)_{op}|6^+)=\frac{1}{\sqrt{2}}b\sum_{\substack{w\,v\\ s}}(-1)^{1-u}\,(-1)^{z}\times$$

$$\times\begin{pmatrix}\frac{9}{2} & \frac{11}{2} & 5\\ w & s & -u\end{pmatrix}\begin{pmatrix}\frac{9}{2} & \frac{9}{2} & 6\\ w & v & -z\end{pmatrix}\hat{6}\,\hat{5}\quad\times$$

$$\times\quad(\phi_{\frac{11}{2}s}(2)|e\,r_2\,Y^*_{1M}(\hat{r}_2)|\phi_{\frac{9}{2}v}(2))$$

$$-\frac{1}{\sqrt{2}}b\sum_{\substack{w\,v\\ s}}(-1)^{1-u}\,(-1)^{z}\begin{pmatrix}\frac{9}{2} & \frac{11}{2} & 5\\ v & s & -u\end{pmatrix}\begin{pmatrix}\frac{9}{2} & \frac{9}{2} & 6\\ w & v & -z\end{pmatrix}\times$$

$$\times\quad\hat{6}\,\hat{5}\,(\phi_{\frac{11}{2}s}(1)|e\,r_1\,Y^*_{1M}(\hat{r}_1)|\phi_{\frac{9}{2}w}(1))\ .$$

Consider the second term in Equation (18). There is a summation over w, v and s and w and v range over the same discrete projection quantum numbers. So in the second term in Equation (18) interchange the summation indices w and v. Then the second term in Equation (18) becomes:

$$\frac{1}{\sqrt{2}}b\sum_{\substack{w\,v\\ s}}(-1)^{1-u}\,(-1)^{z}\begin{pmatrix}\frac{9}{2} & \frac{11}{2} & 5\\ w & s & -u\end{pmatrix}\begin{pmatrix}\frac{9}{2} & \frac{9}{2} & 6\\ v & w & -z\end{pmatrix}\times$$

$$\times\,\hat{6}\,\hat{5}\,(\phi_{\frac{11}{2}s}(1)|e\,r_1\,Y_{1M}(\hat{r}_1)|\phi_{\frac{9}{2}v}(1)).$$

Comparing the above expression with the first term in Equation (18) shows that the only difference between them is that the positions of the w and v are switched in the second 3-j symbol since

$$(\phi_{\frac{11}{2}s}(1)|e\, r_1\, Y^*_{1M}(\hat{r}_1)|\phi_{\frac{9}{2}v}(1)) =$$

$$(\phi_{\frac{11}{2}s}(2)|e\, r_2\, Y^*_{1M}(\hat{r}_2)|\phi_{\frac{9}{2}v}(2)) =$$

$$(\phi_{\frac{11}{2}s}(r)|e\, r\, Y^*_{1M}(\hat{r})|\phi_{\frac{9}{2}v}(r))$$

because the r dependence is integrated over in each case. Using the column permutation property of the 3-j symbol the positions of the v and w can be interchanged as follows:

$$\begin{pmatrix} \frac{9}{2} & \frac{9}{2} & 6 \\ v & w & -z \end{pmatrix} = (-1)^{\frac{9}{2}+\frac{1}{2}+6} \begin{pmatrix} \frac{9}{2} & \frac{9}{2} & 6 \\ w & v & -z \end{pmatrix}$$

$$= -\begin{pmatrix} \frac{9}{2} & \frac{9}{2} & 6 \\ w & v & -z \end{pmatrix} .$$

With the manipulations described above, Equation (18) can be written in the form

$$(19)\quad (5^-|(El)_{op}|6^+) = b\,\frac{1}{\sqrt{2}} \sum_{\substack{w\,v \\ s}} (-1)^{1-u}\,(-1)^{z} \times$$

$$\times \begin{pmatrix} \frac{9}{2} & \frac{11}{2} & 5 \\ w & s & -u \end{pmatrix} \begin{pmatrix} \frac{9}{2} & \frac{9}{2} & 6 \\ w & v & -z \end{pmatrix} \hat{5}\ \hat{6}(\phi_{\frac{11}{2}s}(r)|e\ r\ Y^*_{1M}(\hat{r})|\phi_{\frac{9}{2}v}(r))$$

$$+ b\frac{1}{\sqrt{2}} \sum (-1)^{1-u}\ (-1)^{z} \begin{pmatrix} \frac{9}{2} & \frac{11}{2} & 5 \\ w & s & -u \end{pmatrix} \begin{pmatrix} \frac{9}{2} & \frac{9}{2} & 6 \\ w & v & -z \end{pmatrix} \times$$

$$\times\ \hat{5}\ \hat{6}(\phi_{\frac{11}{2}s}(r)|e\ r\ Y^*_{1M}(\hat{r})|\phi_{\frac{9}{2}v}(r)).$$

Inspection of Equation (19) shows that it is the sum of two identical terms which can be combined. Hence Equation (19) takes a particularly simple form, namely

$$(20)\quad (5^-|(El)_{op}|6^+) = b\sqrt{2} \sum_{\substack{w\ v \\ s}} (-1)^{1-u}\ (-1)^{z}\ \hat{5}\ \hat{6} \times$$

$$\times \begin{pmatrix} \frac{9}{2} & \frac{11}{2} & 5 \\ w & s & -u \end{pmatrix} \begin{pmatrix} \frac{9}{2} & \frac{9}{2} & 6 \\ w & v & -z \end{pmatrix} (\phi_{\frac{11}{2}s}(r)|e\ r\ Y^*_{1M}(\hat{r})|\phi_{\frac{9}{2}v}(r)).$$

The Wigner-Echart theorem (46) gives:

$$(21)\quad (\phi_{\frac{11}{2}s}(r)|e\ r\ Y^*_{1M}(\hat{r})|\phi_{\frac{9}{2}v}(r)) = (-1)^{\frac{11}{2}-s}\ e \begin{pmatrix} \frac{11}{2} & 1 & \frac{9}{2} \\ -s & -M & v \end{pmatrix} \times$$

$$\times\ (n_f\ l_f\ j_f\ ||r\ Y_l||\ n_i\ l_i\ j_i)(-1)^{M}$$

$$= (-1)^{\frac{11}{2}-s} \begin{pmatrix} \frac{11}{2} & 1 & \frac{9}{2} \\ -s & -M & v \end{pmatrix} e(f|r|i)(-1)^{M}(l_f\, j_f||Y_1||\, l_i\, j_i).$$

Combining Equations (20) and (21) gives:

$$(22)\quad (5^-|(El)_{op}|6^+) = b\sqrt{2} \sum_{\substack{w\ v \\ s}} (-1)^{1-u}\,(-1)^{z}\,(-1)^{\frac{11}{2}-s} \times$$

$$\times\ \hat{5}\ \hat{6} \begin{pmatrix} \frac{9}{2} & \frac{11}{2} & 5 \\ w & s & -u \end{pmatrix} \begin{pmatrix} \frac{9}{2} & \frac{9}{2} & 6 \\ w & v & -z \end{pmatrix} \begin{pmatrix} \frac{11}{2} & 1 & \frac{9}{2} \\ -s & -M & v \end{pmatrix} \times$$

$$\times\quad e(f|r|i)\,(-1)^{M}\,(l_f j_f||Y_1||l_i\ j_i).$$

By a series of permutations of the columns of the 3-j symbols this sum over three 3-j symbols can be reduced to a product of a 3-j symbol times a 6-j symbol (47). This fact can be made more evident by writing the matrix element in the following form:

$$(23)\quad (5^-|(El)_{op}|6^+) = e\ b\ \hat{5}\ \hat{6}\ (-1)^{1-u}\,(f|r|i)\,\sqrt{2}\ \times$$

$$\times\quad (-1)^{M}\,(l_f\ j_f\ ||Y_1||\ l_i\ j_i) \times \sum_{\substack{w\ v \\ s}} (-1)^{\frac{11}{2}-s}\,(-1)^{z} \times$$

$$\times \begin{pmatrix} 6 & \frac{9}{2} & \frac{9}{2} \\ -z & v & w \end{pmatrix} \begin{pmatrix} \frac{11}{2} & 5 & \frac{9}{2} \\ -s & u & -w \end{pmatrix} \begin{pmatrix} \frac{11}{2} & \frac{9}{2} & 1 \\ s & -v & M \end{pmatrix}.$$

Now the three 3-j symbols are in the proper form for recoupling the angular momenta through the general identity given below. This identity can be shown to hold by applying the properties of the 3-j symbols to the right hand side so as to obtain an orthogonality relation on two of the 3-j symbols. The general identity is expressed as follows (47):

$$(24)\quad \begin{pmatrix} J_1 & J_2 & J_3 \\ m_1 & m_2 & m_3 \end{pmatrix} \begin{Bmatrix} J_1 & J_2 & J_3 \\ l_1 & l_2 & l_3 \end{Bmatrix} = \sum_{n_1 n_2 n_3} (-1)^{\gamma} \times$$

$$\times \begin{pmatrix} J_1 & l_2 & l_3 \\ m_1 & n_2 & -n_3 \end{pmatrix} \begin{pmatrix} l_1 & J_2 & l_3 \\ -n_1 & m_2 & n_3 \end{pmatrix} \begin{pmatrix} l_1 & l_2 & J_3 \\ n_1 & -n_2 & m_3 \end{pmatrix}$$

where

$$\gamma = \sum_{i=1}^{3} (l_i + n_i).$$

Using Equation (24) to simplify Equation (23) gives:

$$(25)\quad (5^- | (El)_{op} | 6^+) = b\ e\ \hat{5}\ \hat{6}\ (-1)^u\ (-1)^M\ \sqrt{2}$$

$$\times\ (l_f\ j_f\ ||Y_1||\ l_i\ j_i)\ (f|r|i) \begin{pmatrix} 6 & 5 & 1 \\ -z & u & M \end{pmatrix} \begin{Bmatrix} 6 & 5 & 1 \\ \frac{11}{2} & \frac{9}{2} & \frac{9}{2} \end{Bmatrix}$$

where

$$\begin{Bmatrix} J_1 & J_2 & J_3 \\ l_1 & l_2 & l_3 \end{Bmatrix}$$

is known as a 6-j symbol. The values of these 3-j and 6-j symbols are tabulated (48). The physical significance of this matrix element is obtained by squaring it and summing over M and the final state's projection quantum numbers. Thus:

$$(26)\quad \sum_{Mu} |(5^- | (El)_{op} | 6^+)|^2 = \sum_{Mu} b^2\, e^2\, (\hat{5})^2\, (\hat{6})^2\, 2 \times$$

$$\times\, |(l_f\ j_f\ ||Y_1||\ l_i\ j_i)|^2\, |(f|r|i)|^2 \quad \times$$

$$\times \begin{Bmatrix} 6 & 5 & 1 \\ \frac{11}{2} & \frac{9}{2} & \frac{9}{2} \end{Bmatrix}^2 \begin{pmatrix} 6 & 5 & 1 \\ -z & u & M \end{pmatrix} \begin{pmatrix} 6 & 5 & 1 \\ -z & u & M \end{pmatrix} .$$

The summation over M and u can be taken all the way through the expression to the product of the two 3-j symbols where it leads to a value of $\frac{1}{(\hat{6})^2}$ or $\frac{1}{13}$. Thus

$$(27)\quad \sum_{Mu} |(5^- | (El)_{op} | 6^+)|^2 = \frac{1}{13}\, b^2\, e^2\, (\hat{5})^2\, (\hat{6})^2\, 2 \times$$

$$\times \begin{Bmatrix} 6 & 5 & 1 \\ \frac{11}{2} & \frac{9}{2} & \frac{9}{2} \end{Bmatrix}^2 |(l_f\ j_f\ ||Y_1||\ l_i\ j_i)|^2\, (f|r|i)^2 .$$

It can be shown that (49):

$$(28)\quad |(l_f\ j_f\ ||Y_J||\ l_i\ j_i)|^2 = [(-1)^{J+j_i-\frac{1}{2}}]^2 \times$$

$$\times \frac{(\hat{j}_f)^2(\hat{J})^2(\hat{j}_i)^2}{(\sqrt{4\pi})^2} \begin{pmatrix} j_f & J & j_i \\ -\frac{1}{2} & 0 & \frac{1}{2} \end{pmatrix}^2 [\frac{1 + (-1)^{J+l_f+l_i}}{2}]^2 \quad .$$

The wavefunctions are those obtained by solving the Schrodinger equation for a spherical harmonic oscillator single particle Hamiltonian (46), so the radial integrals can be expressed as:

$$(29)\quad (f|r|i) = (n_f\ l_f\ |r|\ \ n_i\ l_i)$$

where

$$\varepsilon_{nl} = (2n + l + \tfrac{3}{2})\ \hbar\ \omega.$$

The $6^+ \rightarrow 5^-$ transition goes between N=5 and N=4 levels since the (1h) and (1g) configurations are involved. Since N = 2n + l, n = 0 for both configurations. It can be shown (49) that

$$(30)\quad (n,\ l+1\ |r|\ n\ l) = (n + l + \tfrac{3}{2})\ r_0$$

where r_0 is the nuclear radius

$$(31)\quad r_0 \simeq 1.1\ A^{\frac{1}{3}}$$

and A is the number of nucleons in the nucleus. In this

particular case:

$$(32)\quad (f|r|i) = (0 \quad 5 \;|r|\; 0 \quad 4) = (0 + 4 + \tfrac{3}{2})^{\frac{1}{2}}\, r_0 = (\tfrac{11}{2})^{\frac{1}{2}}\, r_0 .$$

Combining the various expressions gives upon simplification:

$$(33)\quad \sum_{Mu} |(5^- |(E1)_{op}| 6^+)|^2 = \frac{(25)(3)}{(4\pi)(13)(11)} \times$$

$$\times\, b^2\, r_0^{\,2}\, e^2$$

Therefore the transition probability for the 1.129 MeV $(6^+ \to 5^-)$ transition is given by

$$(34)\quad T(6^+ \to 5^-) = \frac{8\pi}{[(2(1)+1)!!]^2} \left(\frac{1+1}{1\hbar}\right) \left(\frac{1.13}{\hbar c}\right)^3 \times$$

$$\times\, b^2\, r_0^{\,2}\, e^2\, \frac{(25)(3)}{(4\pi)(13)(11)} .$$

Simplifying gives:

$$(35)\quad T(6^+ \to 5^-) = \frac{100}{(3)(11)(13)}\, \frac{1}{\hbar}\, \frac{1.44}{(\hbar c)^3}\, e^2\, r_0^{\,2}\, b^2 .$$

Now consider the 371 keV $(6^+ \to 4^+)$ transition. The transition goes by an E2 multipole and thus the $|4^+)$ state is connected to the $|6^+)$ state by the E2 operator:

$$(36)\quad (4^+|(E2)_{op}|6^+) = \sum_{kl} (-1)^m\, \hat{4} \begin{pmatrix} \frac{9}{2} & \frac{9}{2} & 4 \\ k & 1 & -m \end{pmatrix} \times$$

$$\times \quad \phi_{\frac{9}{2}k}(1)\ \phi_{\frac{9}{2}l}(2)\ \left| \sum_{i=1}^{2} e_i\, r_i^{\,2}\, Y^*_{2M}(\hat{r}_i) \right| \sum_{wv} (-1)^z\, \hat{6} \quad \times$$

$$\times \begin{pmatrix} \frac{9}{2} & \frac{9}{2} & 6 \\ w & v & -z \end{pmatrix} \phi_{\frac{9}{2}w}(1)\ \phi_{\frac{9}{2}v}(2)\ ,$$

which can be simplified to:

$$(37)\quad (4^+|(E2)_{op}|6^+) = \sum_{\substack{kl \\ wv}} (-1)^{m+z}\, e\, \hat{4}\, \hat{6} \begin{pmatrix} \frac{9}{2} & \frac{9}{2} & 4 \\ k & 1 & -m \end{pmatrix} \times$$

$$\times \begin{pmatrix} \frac{9}{2} & \frac{9}{2} & 6 \\ w & v & -z \end{pmatrix} \{\delta_{lv}\ (\phi_{\frac{9}{2}k}(1)|r_1^{\,2}\, Y^*_{2M}(\hat{r}_1)|\phi_{\frac{9}{2}w}(1)) +$$

$$+ \delta_{kw}\ (\phi_{\frac{9}{2}l}(2)|r_2^{\,2}\, Y^*_{2M}(\hat{r}_2)|\phi_{\frac{9}{2}v}(2))\} \quad .$$

Making the same type of manipulations employed previously in connection with Equation (17) gives:

$$(38)\quad (4^+|(E2)_{op}|6^+) = 2 \sum_{klw} (-1)^{m+z}\, e\, \hat{4}\, \hat{6} \quad \times$$

$$\times \begin{pmatrix} \frac{9}{2} & \frac{9}{2} & 4 \\ k & 1 & -m \end{pmatrix} \begin{pmatrix} \frac{9}{2} & \frac{9}{2} & 6 \\ w & 1 & -z \end{pmatrix} (\phi_{\frac{9}{2}k}(r)|r^2\, Y^*_{2M}(\hat{r})|\phi_{\frac{9}{2}w}(r)) \quad .$$

Again using the Wigner-Echart theorem we get the sum over three 3-j symbols as before:

$$(39)\quad (4^+|(E2)_{op}|6^+) = 2\, e\, \hat{4}\, \hat{6}\, (-1)^m\, (-1)^M \times$$

$$\times \sum_{klw} (-1)^{\frac{9}{2}-k}\, (-1)^z \begin{pmatrix} 4 & \frac{9}{2} & \frac{9}{2} \\ -m & k & l \end{pmatrix} \begin{pmatrix} \frac{9}{2} & 6 & \frac{9}{2} \\ -w & z & -l \end{pmatrix} \begin{pmatrix} \frac{9}{2} & \frac{9}{2} & 2 \\ w & -k & -M \end{pmatrix}$$

$$= 2\, (\hat{4})\, (\hat{6})\, (-1)^m\, (-1)^M\, (l_f\, j_f\, ||Y_2||\, l_i\, j_i) \begin{pmatrix} 4 & 6 & 2 \\ -m & z & -M \end{pmatrix} \times$$

$$\times \begin{Bmatrix} 4 & 6 & 2 \\ \frac{9}{2} & \frac{9}{2} & \frac{9}{2} \end{Bmatrix} (f|r^2|i)\, e^2 \,.$$

Hence,

$$(40)\quad \sum_{Mm} |(4^+|(E2)_{op}|6^+)|^2 = \sum_{Mm} e^2\, 4\, (\hat{4})^2\, (\hat{6})^2 \times$$

$$\times\ |(l_f\, j_f\, ||Y_2||\, l_i\, j_i)|^2\ (f|r^2|i)^2 \begin{Bmatrix} 4 & 6 & 2 \\ \frac{9}{2} & \frac{9}{2} & \frac{9}{2} \end{Bmatrix}^2 \times$$

$$\times \begin{pmatrix} 4 & 6 & 2 \\ -m & z & -M \end{pmatrix}^2 \,.$$

The above quantities with the exception of $(f|r^2|i)$ are calculated as previously explained. It is important to note that the initial and final states have the same n and l

values and for this case it can be shown (49) that:

$$(41)\quad (n\ 1\ |r^2|\ n\ 1) = (2n + 1 + \tfrac{3}{2})\ r_0^{\,2}\ .$$

The $(g\frac{9}{2})$ initial and final states require n=0 and l=4. Therefore in the present calculation,

$$(42)\quad (f|r^2|i) = (0\ 4\ |r^2|\ 0\ 4) = (0 + 4 + \tfrac{3}{2})\ r_0^{\,2}$$

$$= \frac{11}{2}\ r_0^{\,2}\ .$$

Thus putting all the calculated values in Equation (40) gives:

$$(43)\quad \sum_{Mm} |(4^+|(E2)_{op}|6^+)|^2 = \frac{(25)^2}{(33)(13)\pi}\ e^2\ r_0^{\,4}$$

Therefore the transition probability for the 0.371 MeV $(6^+\rightarrow 4^+)$ transition is given by:

$$(44)\quad T(6^+\rightarrow 4^+) = \frac{8\pi}{[(2(2)+1)!!]}\ \frac{(2+1)}{2\hbar}\ \frac{(0.371)^5}{(\hbar c)^5}\ \times$$

$$\times\ e^2\ r_0^{\,4}\ \frac{(25)^2}{(33)(13)\pi}$$

Simplifying gives:

$$(45)\quad T(6^+\rightarrow 4^+) = \frac{100}{(99)(13)}\ \frac{1}{\hbar}\ \frac{0.007}{(\hbar c)^5}\ e^2\ r_0^{\,4}$$

The ratio of $T(6^+ \rightarrow 5^-)$ to the $T(6^+ \rightarrow 4^+)$ is given by:

$$(46) \quad \frac{T(6^+ \rightarrow 5^-)}{T(6^+ \rightarrow 4^+)} = \frac{b^2 \frac{100}{(3)(11)(13)} \frac{1}{\hbar} \frac{1.44}{(\hbar c)^3} e^2 r_0^2}{\frac{100}{(99)(13)} \frac{1}{\hbar} \frac{0.007}{(\hbar c)^5} e^2 r_0^4}$$

As stated previously in Equation (31) the nuclear radius r_0 is given by $1.1\ A^{1/3}$. In this case A=90 so $r_0 \approx 4.5$ Fermis. The ratio of transition probabilities is dimensionally correct since the factors $(\frac{E_\gamma}{\hbar c})$ have dimensions $(\text{length})^{-1}$. Using the value

$$\hbar c = 197 \text{ MeV-Fermi},$$

one obtains:

$$(47) \quad \frac{T(6^+ \rightarrow 5^-)}{T(6^+ \rightarrow 4^+)} = 9.6 \times 10^5\ b^2 \ .$$

From the ^{90}Nb decay studies (see Figure 18) the intensity ratio of the two transitions are given by:

$$(48) \quad \frac{I_\gamma(6^+ \rightarrow 5^-)}{I_\gamma(6^+ \rightarrow 4^+)} = \frac{92 \pm 0.5}{1.7 \pm 0.4}$$

Equating these ratios gives b^2 to be:

$$(49) \quad b^2 = (0.56 \pm 0.11) \times 10^{-4} \ .$$

From Equation (14) then:

(50) $a^2 = 1 - b^2 = 0.999944 \pm 0.000011$.

Recalling now that the $|5^-)$ state was written as:

(51) $|5^-) = a[(g\frac{9}{2})(p\frac{1}{2})]_5 + b[(g\frac{9}{2})(h\frac{11}{2})]_5$,

it is clear that the 5^- state is predominantly $[(g\frac{9}{2})(p\frac{1}{2})]_5$. However it is surprising to see that such a small amount of $[(g\frac{9}{2})(h\frac{11}{2})]_5$ configuration added to the $[(g\frac{9}{2})(h\frac{11}{2})]_5$ basic configuration can produce the observed intensity ratio between the 1129 keV $(6^+ \rightarrow 5^-)$ transitions and the 371 keV $(6^+ \rightarrow 4^+)$ transitions.

V. CONCLUSIONS

The three crystal spectrometer proved to be an important instrument for obtaining accurate gamma ray intensities of weak peaks normally masked by Compton background. Conversion coefficients were calculated for 13 transitions from which probable multipolarities were deduced.

Of the levels included in the proposed decay scheme (Figure 18) spins and parities for all but the 4232, 5164 and tentative 5432 keV states were considered known from previous reaction and decay studies (24, 34, 35). The 4232 keV state decays by an E2 or M1 transition to a 5^- level, it is fed by an E1 transition from a 7^+ level, and the log ft value is consistent with first forbidden decay of 8^+ ^{90}Nb, so its spin and partiy must be 6^- or 7^-. The 5164 keV level is fed by allowed electron capture decay of 8^+ ^{90}Nb, it decays via E2 or M1 transitions to 8^+ and 6^+ levels, but it does not feed the negative partiy 4232 keV level. Therefore, the most probable assignments are 6^- for the 4232 keV state and 8^+ for the 5164 keV level.

The 2^+, 5^-, 4^- (at 2738 keV (34), not shown in Figure 18), 4^+, 6^+, 8^+ sequence of states can be described in terms of $(g\frac{9}{2})^2$ and $(p\frac{1}{2})$ $(g\frac{9}{2})$ wave functions (13). However the occurrence of configuration mixing is demonstrated by the 1129 and 1271 keV transitions from the 3448 keV 6^+ and

3589 keV 8^+ level to the 2319 keV 5^- level. The conversion coefficients show these transitions to be E1 and E3 respectively, whereas M4 or E5 is required to connect $(g\frac{9}{2})$ and $(p\frac{1}{2})$ states. It has been shown that 10^{-2}% admixture of $(h\frac{11}{2})$ $(g\frac{9}{2})$ into the wavefunction for the 5^- state explains these data.

VI. LITERATURE CITED

1. Gibson, W. M., Miller, G. L., and Donovan, P. F., in Alpha-, beta- and gamma-ray spectroscopy, edited by K. Siegbahn (North Holland Publishing Co., Amsterdam, 1965), Vol. 1, pp. 345-378.

2. Pell, E. M., Journal of Applied Physics 31, 291 (1960).

3. McKenzie, J. M. and Ewan, G. T. I.R.E. Transactions of Nuclear Science NS-8, 50 (1961).

4. Chasman, C. and Allen, J., Nuclear Instruments and Methods 24, 501 (1963).

5. Heitler, W., The quantum theory of radiation, (Oxford University Press, London, England, 1954), 3rd ed.

6. Freck, D. V. and Wakefield, J., Nature 193, 669 (1962).

7. Tavendale, A. J., Proceedings of the 2nd International Symposium on Nuclear Electronics, Paris, Nov. 1963 (International Atomic Energy Agency, Vienna, in press).

8. Ewan, G. T. and Tavendale, A. J., Canadian Journal of Physics 42, 2286 (1964).

9. Elsasser, W. M., Journal de Physique et le Radium 5, 389 (1934).

10. Mayer, M. G., Physical Review 76, 185A (1949).

11. Haxel, O., Jensen, J. H. D., and Suess, H. E., Physical Review 75, 1766 (1949).

12. Mayer, M. G. and Jensen, J. H. D., Elementary theory of nuclear shell structure (John Wiley and Sons, Inc., New York, N.Y., 1955).

13. Ford, K. W., Physical Review 98, 1516 (1955).

14. Sheline, R. K., Physics 23, 923 (1957).

15. Bayman, B. F., Reiner, A. S., and Sheline, R. K., Physical Review 115, 1627 (1959).

16. Talmi, I. and Unna, I., Nuclear Physics 19, 225 (1960).

17. Auerbach, N. and Talmi, I., Nuclear Physics 64, 458 (1965).

18. Kundu, D. N. and Pool, M. L., Physical Review 76, 183A (1949).

19. Hollander, J. M., Perlman, I., and Seaborg, G. T., Reviews of Modern Physics 25, 469 (1953).

20. Hok, O. P., Kramer, P., and Meijer, G., Physica 20, 1200 (1954).

21. Campbell, E. C., Peelle, R. W., Maienschein, F. C., and Stelson, P. H., Physical Review 98, 1172A (1955).

22. Johnson, O. E., Johnson, R. G., and Langer, L. M., Physical Review 98, 1517 (1955).

23. Lazar, N. H., O'Kelley, G. D., Hamilton, J. H., Langer, L. M., and Smith, W. G., Physical Review 110, 513 (1958).

24. Pettersson, H., Antman, S., and Grunditz, Y., Nuclear Physics A108, 124 (1968).

25. Nordheim, L. W., Physical Review 78, 294 (1950).

26. Nordheim, L. W., Reviews of Modern Physics 23, 322 (1951).

27. Brennan, M. H. and Bernstein, A. M., Physical Review 120, 927 (1960).

28. Cooper, J. A., Hollander, J. M., and Rasmussen, J. O., Nuclear Physics A109, 603 (1965).

29. Dickens, J. K., Eichler, E., and Satchler, G. R., Physical Review 168, 1355 (1968).

30. Vourvopoulos, G. and Fox, J. D., Physical Review 177, 1558 (1968).

31. Martens, E. J. and Bernstein, A. M., Nuclear Physics A117, 241 (1968).

32. Gray, W. S., Kenefick, R. A., and Kraushaar, J. J., Physical Review 142, 735 (1966).

33. Broeck, H. W. and Yntema, J. L., Physical Review 138, 334 (1965).

34. Ball, J. B., Bulletin of the American Physical Society 15, 574 (1970).

35. Ball, J. B., Bulletin of the American Physical Society 14, 545 (1969).

36. Fairstein, E. and Hahn, J., Nucleonics 23, No. 7, 56 (1965).

37. Fairstein, E. and Hahn, J., Nucleonics 23, No. 9, 81 (1965).

38. Fairstein, E. and Hahn, J., Nucleonics 23, No. 11, 50 (1965).

39. Bjornholm, S., Nielsen, O. B., and Sheline, R. K., Physical Review 115, 1613 (1959).

40. Ball, J. B. and Fulmer, C. B., Physical Review 172, 1199 (1968).

41. Taff, L. M. and Champion, P. M., United States Atomic Energy Report IS-1986 (1968).

42. Pettersson, H., Bäckström, G. and Bergman, C., Nuclear Physics 83, 33 (1966).

43. Gunnink, J. B., Niday, R. P., Anderson, R. P., and Meyer, R. A., Lawrence Radiation Laboratory, Livermore, Report UCID-15439 (1969).

44. Sliv, L. A. and Band, I. M., in Alpha-, beta- and gamma-ray spectroscopy, edited by K. Siegbahn (North Holland Publishing Co., Amsterdam, 1965), Vol. 2, pp. 1639-1643.

45. Lederer, C. M., Hollander, J. M., and Perlman, I., Table of isotopes, (John Wiley and Sons, Inc., New York, N.Y., c1967), 6th ed.

46. Roy, R. R. and Nigam, B. P., Nuclear Physics (John Wiley and Sons, Inc., New York, N.Y., 1967).

47. Edmonds, A. R., Angular momentum in quantum mechanics (Princeton University Press, Princeton, New Jersey, 1957).

48. Rotenberg, M., Bevins, R., Metropolis, N., and Wooten, J. K., The 3-j and 6-j symbols (The Technology Press, Cambridge, Massachusetts, c 1959).

49. Cooper, B. S., Nuclear physics 624-625-626, Iowa State University, Ames, Iowa, 1969-1970, (unpublished).

VII. ACKNOWLEDGMENTS

I would like to express my sincere gratitude to Dr. A. B. Tucker for his guidance and encouragement throughout the course of this research, to Dr. Ralph Meeker and Mr. Warren Hein for their invaluable assistance in computer analysis, to Dr. B. S. Cooper for his active interest and assistance in the theoretical calculations, to Dr. A. Bureau, Mr. G. Holland and Mr. J. Sayre of the Synchrotron staff for the sample irradiations. The aid of the above mentioned and all others who in some way helped make this work possible is gratefully acknowledged.